EFFECTS OF DUAL-COOLING ON ANNULAR FUEL NEUTRONIC CALCULATIONS

André Luiz Pereira Rebello Júnior

Dissertação de Mestrado apresentada ao Programa de Pós-graduação em Engenharia Nuclear, COPPE, Universidade Federal do Rio de Janeiro, como parte dos requisitos necessários à obtenção do grau de Mestre em Engenharia Nuclear.

Orientadores: Aquilino Senra Martinez e Alessandro da Cruz Gonçalves

Rio de Janeiro

Março de 2020

EFFECTS OF DUAL-COOLING ON ANNULAR FUEL NEUTRONIC CALCULATIONS

André Luiz Pereira Rebello Júnior

DISSERTAÇÃO SUBMETIDA AO CORPO DOCENTE DO INSTITUTO ALBERTO LUIZ COIMBRA DE PÓS-GRADUAÇÃO E PESQUISA DE ENGENHARIA DA UNIVERSIDADE FEDERAL DO RIO DE JANEIRO COMO PARTE DOS REQUISITOS NECESSÁRIOS PARA A OBTENÇÃO DO GRAU DE MESTRE EM CIÊNCIAS EM ENGENHARIA NUCLEAR.

Orientadores: Prof. Aquilino Senra Martinez

Prof. Alessandro da Cruz Gonçalves

Aprovada por : Prof. Aquilino Senra Martinez

Prof. Alessandro da Cruz Gonçalves

Prof. Zelmo Rodrigues de Lima

Prof. Hermes Alves Filho

RIO DE JANEIRO, RJ - BRASIL

MARÇO DE 2020

Pereira Rebello Júnior, André Luiz

Effects of Dual-Cooling on Annular Fuel Neutronic Calculations/ André Luiz Pereira Rebello Júnior. – Rio de Janeiro: UFRJ/COPPE, 2020.

XIII, 82 p.: il.; 29,7 cm.

Orientadores: Aquilino Senra Martinez

Alessandro da Cruz Gonçalves.

Dissertação (mestrado) – UFRJ / COPPE / Programa de Engenharia Nuclear, 2020.

Referências Bibliográficas: p. 72-76.

1. Combustível anular duplamente refrigerado. 2. PARAGON. 3. Cálculos neutrônicos. I. Aquilino Senra Martinez *et al*. II. Universidade Federal do Rio de Janeiro, COPPE, Programa de Engenharia Nuclear. III. Título.

Acknowledgements

Firstly, I would like to thank my Westinghouse mentor, Dr. Harish C. Huria, for his support, encouragement and assistance during the course of this work. Because of his support, this project could be carried out successfully.

I would also like to thank my UFRJ advisors, Dr. Aquilino Senra Martinez and Dr. Alessandro da Cruz Goncalves, for the guidance and suggestions they have given me in this project and for always believing in me, since my first semester in college.

I very much appreciate the support provided by the Federal University of Rio de Janeiro and the staff of the Nuclear Engineering Program. I'd like to acknowledge the assistance of Liliane Oliveira (Lili) and Reginaldo Baptista (Regis).

A very special gratitude goes out to all at the Westinghouse do Brazil office and my colleagues at Westinghouse Electric Company. With a special mention to my other mentors Rosvita Gold Matthes, Kevin Carl Hoskins and Alexander Pingel; and to my colleagues Glaucia Vinhal Viamonte Cunha, Alice Cunha da Silva, Byron R. Frank, Christopher J. Treleani, David Chan, Petri Forslund Guimaraes and Mohamed Oiusloumen, who in some way were with me during this time.

I also wish to thank Core Engineering & Software Development Department of Westinghouse Electric Company for supporting my research work. I am also grateful to the Westinghouse managers and executives who were involved in the approval of this collaboration: Carlos Leipner, Matthew B. Cerrone, Brian R. Beebe and Michael J. Dembrak.

I wish to also thank Eric S. Gillen and Joseph C. Spadacene for the legal support while establishing the collaboration between Westinghouse and the Federal University of Rio de Janeiro, through the Instituto Alberto Luiz Coimbra de Pós-Graduação e Pesquisa de Engenharia (COPPE).

Finally, I would like to thank my family and my partner Domingos for always supporting me. This journey would not have been possible without them.

Resumo da Dissertação apresentada à COPPE/UFRJ como parte dos requisitos necessários para a obtenção do grau de Mestre em Ciências (M.Sc.)

EFEITOS DE REFRIGERAÇÃO DUPLA NOS CÁLCULOS NEUTRÔNICOS DE VARETA COMBUSTÍVEL ANULAR

André Luiz Pereira Rebello Júnior

Março/2020

Orientadores: Aquilino Senra Martinez
Alessandro da Cruz Gonçalves

Programa: Engenharia Nuclear

Características neutrônicas do combustível anular duplamente refrigerado foram analizadas utilizando um código da Westinghouse para teoria de transporte de nêutrons em duas dimensões baseado em probabilidades de colisão e correntes de interface. Porém, a versão atualmente licenciada do código, PARAGON, tem algumas limitações relacionadas à natureza heterogênea complexa desse combustível. Assim, foi proposto o uso da nova versão do código, o PARAGON2. Atualmente, esta versão se encontra sob extensa validação e qualificação na Westinghouse. O principal uso deste código está na geração de dados nucleares multigrupo de elemento combustível para cálculos no núcleo do reator. O combustível anular duplamente refrigerado é refrigerado tanto nos canais de refrigeração interno e externo da vareta de combustível. Este novo design de combustível foi proposto para permitir um aumento de potência no combustível ao mesmo tempo que mantém ou melhora os limites de segurança. Revisão bibliográfica evidenciou a carência de códigos de transporte capazes de modelar este combustível com precisão aceitável. Isso se deve ao fato de que as relações de equivalência para as integrais de ressonância em meio heterogêneo adotadas nos códigos usuais foram formuladas apenas para varetas cilíndricas sólidas. O objetivo deste estudo é validar o uso do software PARAGON2 para modelar o combustível anular duplamente refrigerado. Tal validação será com simulações MCNP. Tanto os modelos de vareta como de elemento combustível serão modelados.

Abstract of Dissertation presented to COPPE/UFRJ as a partial fulfillment of the requirements for the degree of Master of Science (M.Sc.)

EFFECTS OF DUAL-COOLING ON ANNULAR FUEL NEUTRONIC CALCULATIONS

André Luiz Pereira Rebello Júnior

March/2020

Advisors: Aquilino Senra Martinez
Alessandro da Cruz Goncalves

Department: Nuclear Engineering

Neutronic characteristics of the dual cooled annular fuel were analyzed using the Westinghouse two-dimensional transport theory code based on collision probabilities and interface currents. However, the current licensed version of the code called PARAGON has some limitations for the complex heterogeneous nature of these assemblies. It was thus proposed to use a newer version of the code called PARAGON2. At present, this is under extensive validation and qualification in Westinghouse. The main usage of this code is on the generation of the multi-group nuclear fuel assembly data for reactor core calculations. The dual-cooled annular fuel is cooled in both internal and external cooling channels. This new fuel design was proposed to allow an increase in power density while maintaining or improving safety margins. Bibliographical review showed there is a lack of transport codes capable to model such fuel with acceptable accuracy and validated for this purpose. This is because the equivalence relations for heterogeneous resonance integrals adopted in the standard codes were formulated only for solid cylindrical rods. The purpose of this study is to validate the usage of PARAGON2 code to model dual-cooled annular fuel. This validation will be done with MCNP. Both pin and assembly models will be modeled.

List of Abbreviations and Acronyms

ANC – Advanced Nodal Code

ATF – Accident Tolerant Fuel

C* – Conversion Ratio

CANES – Center of Advanced Nuclear Energy Systems

CFD – Computational Fluid Dynamics

DCF – Dual-Cooled (Annular) Fuel

DNB – Departure from Nucleate Boiling

DNBR - Departure from Nucleate Boiling Ratio

ENDF – Evaluated Nuclear Data Files

HFP – Hot Full Power

HZP – Hot Zero Power

IFBA – Integral Fuel Burnable Absorber

K_∞ – Infinity Neutron Multiplication Factor

KAERI – Korea Atomic Energy Research Institute

LOCA – Loss of Coolant Accident

MCNP – Monte Carlo N-Particle

MDNBR – Minimum Departure from Nucleate Boiling Ratio

MIT – Massachusetts Institute of Technology

MOX – Mixed Oxide Fuel

MWd/kgU – Megawatt Days per kilogram (Uranium/Metal)

MWth – Megawatt Thermal

NERI – Nuclear Energy Research Initiative

NRC – Nuclear Regulatory Commission

OD – Outer Diameter

OFA – Optimized Fuel Assembly

pcm – Percent Mille

ppm – Parts per Million

PWR – Pressurized Water Reactor

RFA – Robust Fuel Assembly

TRL – Technology Readiness Level

UFEML – Ultra-fine Energy Mesh Library

VVER – Water-Water Energetic Reactor

Table of Contents

List of Tables

List of Figures

1 Introduction and Background

1.1 Introduction

In the last decades, huge effort has been invested into improving performance of PWR fuels and increasing nuclear power plant economy. In a reactor, the fuel pellet is the source of power, as the heat generated in it is transferred to the surface of the cladding where the coolant removes and carries it to electrical generators. Being such a crucial point, it is surprising how most of the efforts done were focused on improving the material properties while maintaining the pellet geometry almost unaltered. Aiming for a more innovative fuel design change with minimum modifications to the plant design, the Dual-Cooled annular Fuel (DCF) concept has been proposed.

The Dual-Cooled Fuel is composed of internal and external cladding tubes in which annular fuel pellets are stacked and cooling water flows in both external and internal channels [1]. With that, the DCF has two cooling surfaces: the inner cladding in contact with the coolant flowing in the inner channel and the outer cladding in contact with the coolant flowing in its surroundings. Figure 1.1-1 illustrates this fuel concept. Due to the thin pellet thickness and increased heat transfer area, this design allows for an increase in core power density while maintaining or improving safety margins.

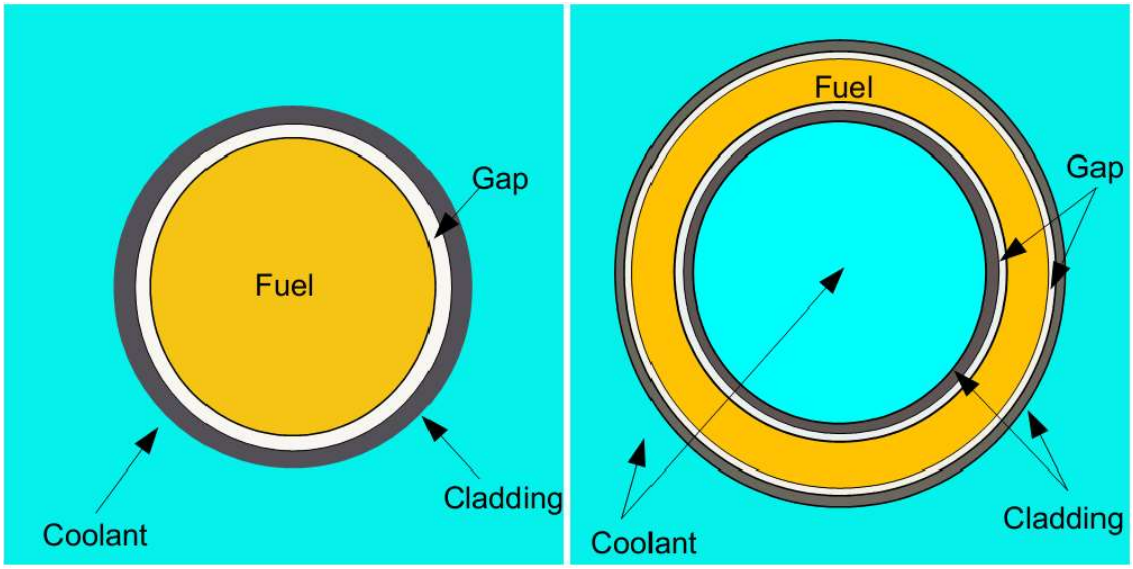

Figure 1-1: Schematics of solid and dual-cooled annular fuel (not to scale) [2]

In fact, the annular fuel is not a brand-new idea. The first concept of internally and externally cooled annular fuel had been suggested by R. Bujas for high temperature gas cooled reactors back in 1971 [3]. Since then, annular fuel has been studied and several types of annular fuels were tested and used in different type of reactors. Due to the lack of in incentive to pursue this type of research, however, the concept was put aside either because of economic reasons or technological limitations. Given that the energy economics in the world has been changing, reflecting a strong competition between nuclear energy and other power sources, the nuclear industry has now shown more interest in the concept of annular fuels [2].

A new wave of studies on dual-cooled annular fuel started when the U. S. Department of Energy, under the Nuclear Energy Research Initiative (NERI) program, funded a research on internally and externally double-cooled annular fuel for advanced PWRs, aiming to endure a substantial power uprate. This research was leaded by the Center of Advanced Nuclear Energy Systems (CANES) of the Massachusetts Institute of Technology (MIT) and had contributions from Westinghouse (which brought in INVAP and CNEA), Gamma Engineering, Framatome and Atomic Energy of Canada. As an outcome of this project, Reference [4], which is further reviewed in Section 2, was issued.

The dual-cooled annular fuel was proposed by MIT to allow a substantial increase in power density (on the order of 30% or higher) while maintaining or improving safety margins. The report evaluated the performance of this fuel from many perspectives: Thermal hydraulic performance, Safety Analysis performance, Neutronic performance, Fuel Fabrication Feasibility, Economic Feasibility and Fuel Performance.

As described in Sections 2 and 5, the Reactor Physics section of the report proposed two annular fuel lattices. These geometries served as a basis for the work performed in this study.

The report also exposed the lack de neutronic codes capable and verified for modeling this type of fuel. The reason for this is that the equivalence relations for heterogeneous resonance integrals adopted in the usual codes were formulated only for solid cylindrical rods. Hence, this study was proposed to not only evaluate the Reactor Physics aspect of the dual-cooled annular fuel using PARAGON2, but also to provide means of assessing the code's ability of modeling this new fuel design.

PARAGON2 is the new version of the PARAGON code, which is the current Westinghouse lattice code used for PWRs. The code is still undergoing the NRC licensing process. PARAGON2 employs an Ultra-Fine Energy Mesh Library (UFEML) with 6064 neutron and 97 gamma energy groups for multi-group cross section calculations, which is expected to allow the code to be used for any fuel assembly type, regardless of the design complexity, as it eliminates the need for the resonance self-shielding calculation.

1.2 Background information

After the Fukushima accident, the vulnerabilities of current fuels to LOCA (Loss of Coolant Accidents) were highlighted. This prompted efforts throughout the world to develop fuels that are more accident tolerant and that could be used in both current and new build reactors. Thus, the idea of Accident Tolerant Fuel (ATF) was created.

The objective of ATF would be to tolerate higher temperatures, to reduce exothermic oxidation in water/steam and associated generation of potentially explosive hydrogen gas, to increase "grace period", and to provide an economic benefit, if possible (or at least not a significant detriment) [5].

To achieve this objective, two characteristics can be changed: the UO_2 fuel and the Zirconium Clad. Several concepts of ATF were proposed with different ways of changing these two parameters. Some of these are depicted in Figure 1-2.

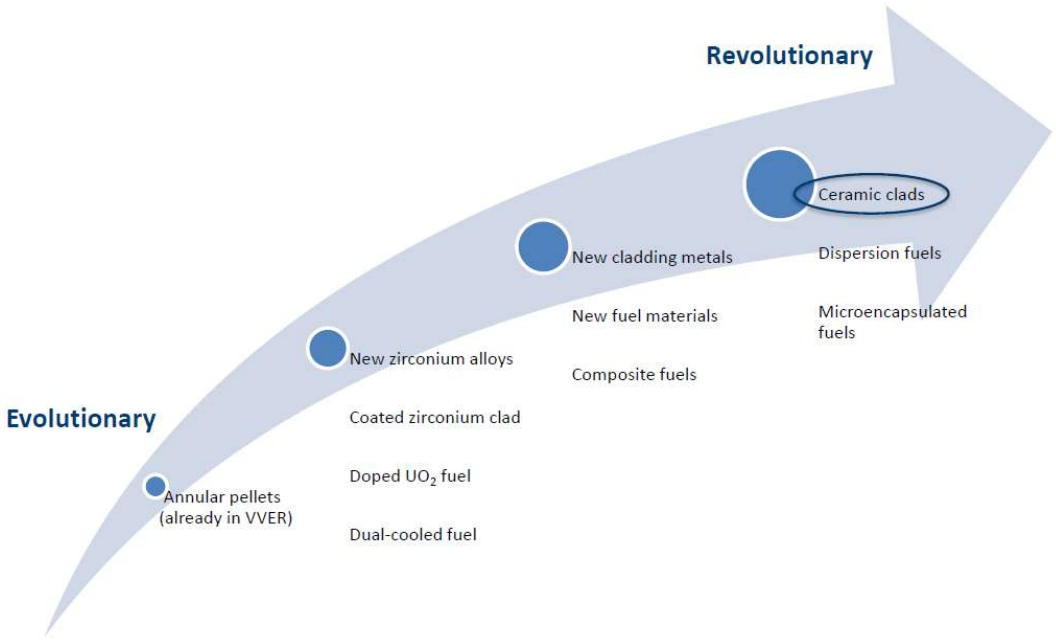

Figure 1-2: Different concepts proposed for Accident Tolerant Fuel [5]

The dual-cooled fuel fits into the "Geometric Changes" category of ATF concepts. Reference [5] lists its advantages as the safety margin increase and the possibility of power uprate, which would bring economic benefit. As disadvantage, the difficulty of manufacturing the annular region within the tolerances is listed.

Reference [6] assesses the Technology Readiness Level (TRL) of a broad range of potential advanced nuclear fuel concepts relevant for Generation III, III+, IV and Small Modular Reactors (SMRs), including those considered to be potential ATFs. In this study, the DCF is categorized with a TRL of 5 out of 10. This TRL is described as the technologies which have the basic system successfully demonstrated. For the DCF fuel, this level was based on the fact that test rods were already irradiated in Korean commercial PWRs [7].

While the MIT project had as a reference plant the standard Westinghouse PWR, the Korea Atomic Energy Research Institute (KAERI) started their efforts focusing on the OPR-1000, which is the standard Korean PWR. Several researches have been carried out by the Korean scientists lately in this topic and test rods were even irradiated already.

Another line of study which emerged was considering modifying a typical VVER-1000 reactor to use dual-cooled annular fuel. Given that the standard VVER-1000 pellet is annular, a shift to dual-cooled annular fuel could be less revolutionary.

Finally, research has also been done considering more advanced reactor generations. The dual-cooled annular fuel was proposed for Small Modular Nuclear Reactors (SMRs) and even for the Supercritical Water-Cooled Reactor (SCWR). All of these studies will be further reviewed in Section 2.

1.3 Research objectives

The main objective of this dissertation is to study of the effects dual-cooling in fuel assembly neutronics using PARAGON2 and MCNP and to assess PARAGON2's ability of modeling dual-cooled annular fuel.

1.4 Dissertation outline

Chapter 2 presents a bibliographical review on annular nuclear fuel covering different perspectives.

Chapter 3 describes the PARAGON code, its new version PARAGON 2 and its improvements, and how it is situated in the NEXUS/ANC9 code system used by Westinghouse.

Chapter 4 covers the MCNP code, which will be used to create benchmarks for the PARAGON2 validation.

Chapter 5 describes how the validation will take place and how the modelling will be done, including the assumptions, modeling differences and referenced data which can be used as acceptance criteria.

Chapter 6 presents the results.

Chapter 7 summarizes the conclusions and envisions the potential future work.

2 Literature Review

This section presents a literature review of relevant analyses carried out to study the dual-cooled annular fuel from different perspectives: Thermal hydraulics, Safety Analysis, Manufacturing and, finally, Reactor Physics, which is the focus of this study.

2.1 Thermal-Hydraulics

Reference [8] documents the thermal hydraulics analysis of dual-cooled fuel applicable to the reference PWR. The study was focused on steady-state thermal-hydraulics performance aiming to identify the optimum geometry and the magnitude of the potential power density increase of the traditional PWR cores with solid rods. The selected base case for this study was a typical Westinghouse 3411 MWth four loop PWR plant.

The study started with an exploratory analysis of the DCF using one-rod model to identify the dimensions that would result in a flow split that produces the largest MDNBR. The coolant flow split was calculated using the in-house computer code TAFIX (Thermal-Hydraulic Model of Annular Fuel with Internal and eXternal Cooling). Then the heat transfer from the fuel rod to the cladding was computed using the RETRAN computer code.

Several assumptions were adopted when performing the exploratory analysis to find the optimum dimensions of the annular fuel pin and array size. The overall dimensions of the annular fuel assembly were assumed fixed equal to those of the reference 17x17 bundle with solid fuel pins. Array sizes ranging from 11x11 to 15x15 were analyzed. The analysis assumed 18% power uprate, to allow for any transient. Among other assumptions, the inner and outer cladding thicknesses were assumed identical and equal to that of the cladding of a solid pin in the Westinghouse 17x17 array.

It was observed that the smaller is the assembly size, the higher is the peak temperature. As the number of fuel rods in the assembly decreases, the rod linear heat rate increases for a fixed assembly power, which results in a higher peak temperature. Despite that, all annular peak fuel temperatures were still below those of the solid fuel case.

It was also observed how the MDNBR is affected by the array size. For the arrays with larger number of fuel rods, the MDNBR occurs in the inner channel. By reducing the number of fuel rods, the inner channel diameter increases, which allows for more flow and shifts the MDNBR for the outer channel. The maximum DNBR margin was found for the 13x13 array.

Another parameter studied was the core pressure drop at 100% power. Due to the smaller hydraulic diameter of the coolant channels, the pressure drop increases with the number of rods in the assembly. Beyond 13x13, the array sizes showed a large increase of pressure drop. In addition, the pressure drop of 13x13 array was found to be close to that of the reference 17x17 PWR fuel.

From these three analyses, the study concluded that the 13x13 design was the optimum configuration and thus selected it to be further analyzed.

The 13x13 lattice was then analyzed in a one rod model using VIPRE-01/Mod2 (Versatile Internals and Component Program for Reactors; EPRI) [9]. The option in this code of calculating the heat conduction in hollow tubes was used to model DCF. One rod model results agreed well with the TAFIX results for flow rate, pressure drop and DNBR; which confirmed the accuracy of the hollow tube option for this purpose.

VIPRE-01 was then used for whole-core modeling of the 13x13 lattice, in order to obtain more realistic and accurate MDNBR. The results showed a large difference from what was previously calculated in the one-rod model. Due to that, the study partially repeated the optimization study, now using the whole core model also for the 12x12 and the 14x14 arrays.

Based on MDNBR, the most promising options were found to be the 13x13 and the 12x12 arrays. Since the 13x13 array was able to accommodate a higher heat flux to the outer channel, it was selected as the most promising one. This design allowed for a power uprate of 50% in terms of DNBR limit, assuming the same core volume as the reference solid fuel at 100% power. In addition, the power uprate would be possible with fuel peak temperatures substantially below the reference solid fuel, reducing gas release and improving LOCA performance.

In addition, it was also evaluated the sensitivity of MDNBR to different parameters and tolerances. MDNBR was identified to be more sensitive to gap

conductances in the inner and outer gaps, which would require more experimental investigations.

Finally, one issue pointed out was the need for an increase of flow rate from the reactor circulation pumps to maintain the core temperature rise. The 50% power uprate was found possible reducing the inlet temperature by 10°C when using the largest available pumps with double the power of current pumps but smaller flow rate than 150%. DCF was also found to be resistant to flow instabilities.

All the aforementioned results are also presented at the Section 6 of the NERI report [4].

Another thermal-hydraulic analysis was performed in Reference [10], where Kwon et al compared the characteristics of solid type and annular type nuclear fuel pellet under the same conditions using the finite element program of thermoelastic-plastic-creep analysis. They concluded that the maximum temperature achieved by the annular fuel was 835.5 °K, which is less than half of the one exhibited by the solid fuel, 2086.7 °K, for the same overall heat generation. This temperature difference means that there's more margin in the case of an accident in the plant. In case of a LOCA event, for instance, the critical time of melting for the annular fuel is much longer than that of the solid fuel. In addition, the maximum hoop stress in the pellet of the annular type was 94.7 MPa, which is less than 10% of the one in the solid type, 1130.7 MPa, reducing the chance of pellet fracture that could lead to tear of the cladding. From these findings, the study concluded that the annular fuel operation is safer than the solid fuel for the same overall heat generation or that the annular fuel can produce higher power maintaining the same level of safety as in the solid fuel.

Several studies have proposed adapting a typical VVER-1000 reactor to use dual-cooled annular fuel.

Reference [11] investigated both DCF and solid fuel pins in the VVER-1000 reactor using MCNP5 to obtain neutronics parameters of the core. In parallel, pitch optimization was performed for each annular case to obtain the best configuration and dimension. With the neutronic parameters, power peaking factors of the fuel assemblies and the heat flux of hottest fuel rods were determined, for then the MDNBR to be calculated. Results concluded that annular fuel rods have margin available on MDNBR

in both inner and outer surfaces relative to solid fuel. In conclusion, the study proposed an annular pin configuration as the best option based on the investigations carried out.

Reference [12] analyzed the usage of dual-cooled annular fuel in the VVER-1000 reactor from a thermal hydraulics perspective, using K–ω SST Turbulence model, aiming to estimate the amount of thermal power uprate that would be viable. For this, the pitch length of fuel rods was designed. Then a fuel rod in hot channel was simulated by CFD codes to perform thermal-hydraulic calculations and compare them to conventional VVER-1000 without the dual-cooled fuel. Results showed enough margin available fuel pellet temperature and DNB to accommodate a 129% power uprate.

Reference [13] went even further and proposed a Thorium-based dual-cooled fuel for the VVER-1000 reactor. Thermal performance of this core was analyzed using ANSYS CFD code. Maximum fuel and clad temperatures were estimated using an equivalent cell that includes both the fuel rod and the coolant within the hexagonal assembly in the hot channel. While the Uranium-based fuel reached a maximum temperature of 1370 K, the Thorium-based temperature was 840K. In addition, it resulted in a flatter power distribution in the reactor core. Critical Heat Flux (CHF) and minimum DNBR are obtained and validated. With that, it was concluded that the thorium-based dual-cooled fuel provided more thermal safety margin in the reactor than the conventional UO_2 fuel.

Finally, Reference [14] describes the thermal-hydraulics design of a Small Modular Reactor (SMR) with a core using 13x13 fuel assemblies with fully ceramic micro-encapsulated (FCM) and annular fuel rods. The subchannel analysis code MATRA, which was developed by KAERI, was used to perform this analysis. MDNBR, fuel temperature and Available Overpower Margin were evaluated. When comparing to conventional PWR, the FCM annular fuel was estimated to provide an improvement of thermal margin with 30% as well as a fuel centerline temperature with 50%.

2.2 Safety Analysis

References [15, 16] documents the safety analysis study of DCF in a 4-loop PWR for the following transients and accidents: Loss of Flow Accident (LOFA), Main Steam Line Break (MSLB), Large Break Loss of Coolant Accident (LBLOCA) and Rod Ejection Accident (REA). This study was performed using RELAP5 and VIPRE codes. It was

found that the minimum DNBR for the annular fuel at 150% power never dropped below the minimum DNBR value for the reference solid fuel at 100% power for LOFA and MSLB transients. For the LBLOCA transient, several options for safety injection flow rates and accumulator size were analyzed and the reflood models were applied separately to the inner and outer surfaces. In all cases, the temperatures with the uprate were below the regulatory limit. For the REA analysis, the enthalpies and temperatures were much smaller for the annular fuel, both at 100% and 150% power, compared to the ones for the solid fuel at 100% power. These results indicated that this fuel would be able to accommodate a 50% power uprate in a PWR and still maintain adequate safety margins for the analyzed transients. These results are also presented at the Section 7 of the NERI report [4].

2.3 Manufacturing

Reference [17] assessed the viability of the dual-cooled fuel manufacturing. Five fabrication routes and processing technologies were evaluated. Two routes were identified as the most promising: the sintered ring pellet fabrication route using current pinch and die pressing technology for fabricating green pellets, followed by sintering and grinding; and the VIPAC fuel element fabrication route with different particle size components of crushed high density sintered UO_2 fuel material. These two routes were further analyzed and developed.

The study then performed laboratory-scale demonstration of the developed processes to provide near prototypical annular fuel rods with depleted uranium oxide for pertinent product characterization.

Using the VIPAC approach, first six 10cm long annular fuel specimens were fabricated by AECL to be used at MITR for irradiation. These are depicted in Figure 2-1. Difficulty was found on obtaining a high UO_2 density using the VIPAC approach for longer fuel. Two four-foot lengths of annular fuel were manufactured to achieve a maximum density of 77% if theoretical, which is insufficient to meet the requirements of at least 85%. However, it was noted that higher densities may be achieved through an addition of a uranium metal powder component to the oxide fuel mixture before compaction.

Figure 2-1: Six 10cm long annular specimens fabricated by AECL using VIPAC approach [4]

Then, following the sintering route, sintered ring pellets for the 13x13 array were manufactured at the Westinghouse facility in Columbia, South Carolina, United States. Some of these are shown in Figure 2-2. The sintered pellets were extensively measured and evaluated and no technical issues with the fuel pellet fabrication or OD surface grinding were found. The pellet dimensional tolerance met the preliminary fuel design specifications. With that, the press-and-sinter pellet fabrication route was identified as the most promising technology for commercially manufacturing DCF, from the ones analyzed. A second batch of about 200 pellets was then manufactured at INVAP (located in S. C. de Bariloche – Rio Negro Province, Argentina), showing that the tolerances can be achieved. Finally, four-foot log rods were loaded with the pellets and the end plugs were welded, showing that annular fuel elements can be manufactured by commercial fabrication techniques.

These results are also presented at Section 11 of the MIT report [4].

Figure 2-2: Annular pellets manufactured by Westinghouse using sintering process [4]

The Korea Atomic Energy Research Institute (KAERI) has also developed many technologies for the dual-cooled fuel. Reference [7] discusses some of these technologies. A feasibility study was done on using dual-cooled annular fuel in the Korean standard PWR (OPR-1000) for a 120% power uprate, while keeping their current 16x16 guide tube layout, which would avoid any change in reactor internals related to control rod driving system.

Manufacturing technology of annular fuel pellet and cladding was developed to fabricate annular pellets with precisely controlled inner diameter without inner surface grinding. This precision is needed as it relates to the inner and outer gap thicknesses, which then relate to the gap conductance that affects the heat flux split toward both internal and external cladding. The developed technology uses a precisely machined rigid rod as inner surface deformation stopper during the sintering process. More on the three fabrication approaches investigated by KAERI can be found on Reference [18].

Finally, Reference [7] also discusses the fuel performance and irradiation test results. For these, six test rods were manufactured and irradiated at the research reactor HANARO during 100 effective full power days. Due to the low fuel pellet temperature, smaller solid swelling rate (0.25~0.60 vol% per 10 MWd/kgU) was obtained compared

to average one for commercial solid UO_2 pellet. KAERI also proposed a technology for handling with inner channel blockage, which is an important technical issue as the inner channel of the dual-cooled fuel is isolated from the outer channel. The technology is based on making several side orifices on a cylindrical wall of the lower end plug, so that coolant from the inner channel could be supplied through them.

2.4 Reactor Physics

Reference [19] documents the reactor physics performance of typical PWR cores fueled with dual-cooled annular fuel while comparing them to reference solid fuel.

Firstly, lattice physics benchmarks were performed by modeling pin cell models in CASMO-4 [20] and comparing them against the Monte Carlo burnup code package, MCNP-4C/ORIGEN-2.1/MCODE-1.0. CASMO-4 is the lattice physics code of the licensing-level Studsvik Scandpower core management system. Benchmarks were calculated for a typical Westinghouse PWR 17x17-lattice solid fuel design and two annular fuel designs. The two annular fuel designs were: the 13x13 lattice (labeled as PQN-02), which was the most promising from the Thermal-Hydraulics analysis, as described in Section 2.2; and the 15x15 lattice (labeled as PQN-01). The difference between CASMO-4 and the Monte Carlo package for the standard solid fuel was taken as a reference for the comparison of the annular fuel results.

It should be noted that the MCODE-1.0 calculations adopted continuous energy library based on the ENDF-V library, the used CASMO-4 was based on 70-group cross section libraries processed from JEF-2.2 libraries. Such library difference was expected to cause an almost constant eigenvalue difference in the solid fuel results.

Several assumptions were taken. For all assembly, even the ones with annular fuel, the overall assembly size was assumed the same as the typical PWR 17x17 assembly. All calculations were poison-free: no burnable poison nor soluble poison (Boron). The fuel was UO2 at 4.95 w/o enrichment and 95% theoretical density and periodic boundary conditions on all edge surfaces. Hot operation conditions were assumed at a core power density of 104.5 kW/liter-core. The solid fuel temperature is modeled as 900 K while the annular fuel temperature is set to 600 K. In all cases, water is modeled at 583.1 K. The assumed geometric dimensions are reproduced in Table 5-1.

The models were benchmarked at Beginning of Life (BOL) conditions with respect to the conversion ration (C*), which is defined as the ratio of U-238 capture rate to U-235 fission rate, and the eigenvalue. In both cases, the deviations were considerably smaller for the solid fuel than for the annular fuel lattices. The deviation in C* for the annular fuel indicates that CASMO-4 underestimates the U-238 capture rate, which would lead to the observed higher eigenvalues compared to MCNP-4C predictions. The resonance calculation was identified as the reason for U-238 capture rate being underestimated. The provided justification follows:

> *"Due to the water presence inside of the annular fuel, the self-shielding effect is reduced and U-238 resonance captures are effective on both sides of the annular fuel pellet. However, equivalence relations for heterogeneous resonance integrals were formulated only for solid cylindrical rods in the CASMO-4 resonance calculations, i.e., CASMO-4 assumes epithermal U-238 captures to occur only at the outer surface of the annular fuel pellet. Thus, the resonance integrals are inadequate for annular fuel and are responsible for the underestimate of U-238 capture rates".* [19]

With that, it was concluded that the CASMO-4 code needed to be improved for modeling dual-cooled annular fuel. Ways of remediating the issue by doing adjustments in CASMO-4 without changing the source code were described.

Three ways were proposed for the poison-free pin cell fuel: fictitious increasing the U-238 number densities to increase the epithermal U-238 captures; fictitious reducing the coolant density to reduce moderation; and adding a small amount of Hafnium to dampen reactivity. A 20% increase in the U-238 content seemed to be the best option.

For the case of a fuel poisoned with Gadolinium, it was observed that a 30% increase in U-238 content would give the best agreements.

The adjustment results from the poison-free and the Gadolinium-poisoned pin cell models were combined in a full fuel assembly model. The results for eigenvalues as a function of burnup indicated that this approach is acceptable.

The next step of the study was to evaluate the neutronic characteristics of the annular fuel. For that, the differences between the solid fuel rod and the dual-cooled annular fuel rod were analyzed in a step-by-step basis. Neutronic parameters were calculated for several cases that cover from the reference solid pin to the DCF in step-by-

step changes, as shown in Figure 2-3. It was observed that the geometry effect was the most important one, which significantly increases the resonance absorption of fuel due to the increase in fuel surface-to-volume ratio.

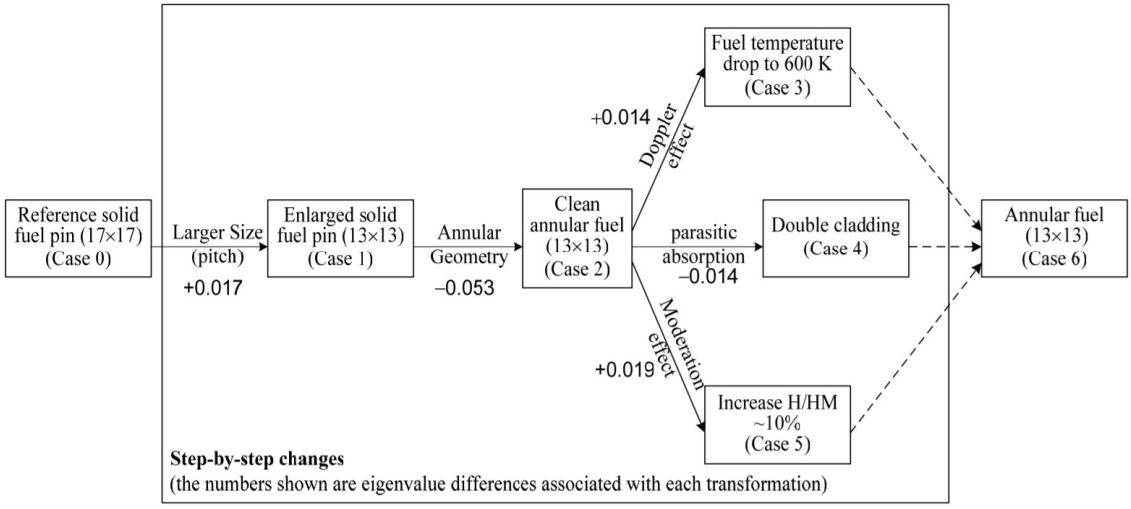

Figure 2-3: Illustration of step-by-step changes from solid fuel to dual-cooled annular fuel [19]

The next step of the study was to perform lattice burnup calculations. It was observed a similar burnup capability between the solid and the annular fuel designs for the same enrichment. However, the annular design requires an increase in enrichment to match the same energy production of the solid one due to the reduce fuel volume.

Finally, equilibrium PWR core designs were modeled for 3 cases: solid reference core, annular core at full power and annular core with 50% power uprate. The reference core is an equilibrium Westinghouse 4-loop 18-month-cycle PWR model with a rated thermal power of 3411 MWt. The steady-state core performance and reactivity feedback parameters in the annular fuel cores were found to be very similar to the reference solid one. With that, all the imposed design targets were met for them.

All the aforementioned neutronic results are also presented at Section 9 of the NERI report [4].

Reference [21] documents both the thermal-hydraulics and neutronic analyses of DCF for a power uprate in a VVER-1000 reactor. Neutronic calculations were performed using both deterministic codes (WIMS and CITATION) and a stochastic code (MCNP-4C). Clean and cold conditions and a temperature of 300 K were assumed. The core of a

conventional VVER-1000 was modeled. Curves of the variation of the effective core multiplication factor relative to the pitch length of the fuel rods were modeled in both codes. Two pitch lengths (15.88 and 23mm) for the annular fuel were identified by setting the multiplication factor to be the same as the conventional reactor (k_{eff} = 1.27768). However, only one of these (15.88mm) were in the under moderated zone and thus was selected as the appropriate pitch length. In addition, the results for the pitch length showed a 1.133% relative error between the deterministic and stochastic codes.

Reference [22], on the other hand, studied the fuel assembly neutronics of DCF in a Supercritical Water-Cooled Reactor (SCWR), using the code FENNEL-N, which is based on the advanced lattice code HELIOS and the core-wise nodal diffusion code SIXTUS. FENNEL-N results were validated by comparison against MCNP using ENDF/B-VI cross-section library. It was observed that traditional assembly homogeneous method introduced a large error due to the difference between PWR spectrum and SCWR spectrum. The keff results showed a maximum of 687 pcm relative error. The radial power distribution results had a maximum of 8.37% relative error, in the assembly periphery. When applying a change in the energy spectrum, the maximum error in pin power distribution was reduced to a magnitude of 1.70%.

3 PARAGON Code

The current section focusses on the PARAGON2 code, which is the proposed code in this dissertation to model dual-cooled annular fuel.

Section 3.1 describes the NEXUS system where the PARAGON code is situated. Section 3.2 reviews the methodologies and modules present in the code. Section 3.3 briefly describes the process followed for the code qualification. Finally, section 3.4 goes over the new version of the code, PARAGON2, and its differences when compared to the first version.

3.1 NEXUS System

NEXUS is an automated once-through cross section system designed to provide nuclear data to core simulators. NEXUS has been implemented, qualified, and licensed for PWR core analysis in the United States [23,24]. It accurately and efficiently models and predicts core performance for all square lattice PWRs.

The NEXUS code system is used to generate cross-section data files for the core simulator, ANC9. These data files are generated only once for each unique fuel region of fuel and include a full range of fuel and moderator temperature, burnups, and other core conditions for modeling the fuel throughout its lifetime in the reactor.

The PWR NEXUS system consists of several computer codes: NEXrun, NEXpre, ALPHA, PARAGON, NEXlink and ANC9. These are briefly described below and interface according to the flowchart in Figure 3-1.

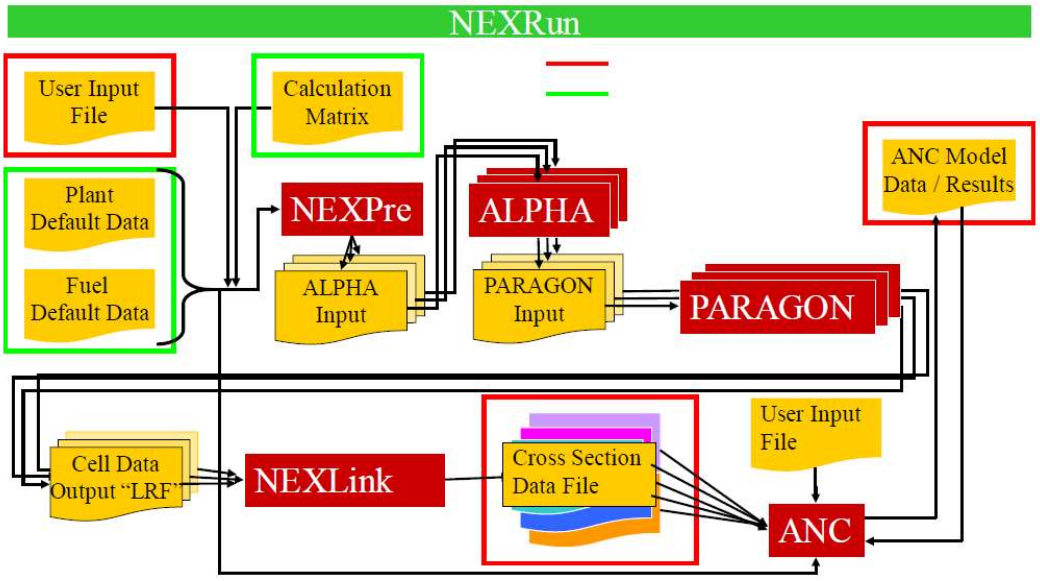

Figure 3-1: Flowchart for the NEXUS system [25]

- NEXrun is the overall system controller, which allows for the running of the NEXUS system to be fully automated. This program executes each of the subsequent codes and controls the data transfer between these codes. For typical production calculations, the user only needs to provide the NEXpre input and execute NEXrun to obtain cross sections for the core simulator (ANC). At the conclusion of NEXrun execution, the cross section data file will be generated and ready for use with the core simulator.

- NEXpre works together with ALPHA to provide the user input interface with the code system and generate all the input necessary for the lattice code, considering a matrix of calculations that need to be performed to cover all the conditions needed for the once-through cross-section data files. NEXpre is linked to a controlled database which supplies most of the data needed to develop the lattice code input including cycle specific fuel and plant data from the Westinghouse database of cores and reload information, material and fuel information based on their thermo-mechanical properties and expected irradiation behavior. In typical production calculations, the NEXpre input file is very simple and limited to data specific to a given fuel type, though flexibility is provided to suit the needs of development applications.

- PARAGON is the Westinghouse lattice transport code used to generate the lattice nuclear data. PARAGON was licensed in the U.S. in 2004 [26] and is also used in PWR nuclear design as part of the Westinghouse APA nuclear code system (ALPHA/PHOENIX-P/ANC), where it replaces the PHOENIX-P code. More details on PARAGON and its new version, PARAGON2, are given in the other subsections of this section.
- NEXlink is the implementation of the NEXUS cross section representation methodology, processing the nuclear data from the lattice codes and generating the fitted data and other nuclear data needed by the simulator. NEXlink as been written in a general manner. The user does not have to input any details about the calculation matrix that NEXlink will fit. NEXLink determines the details of the calculations that it is being asked to fit at runtime. NEXlink generates backfitting statistics to keep the user informed as to the quality of the fitting. NEXlink writes the final fitting data as well as pin data and other nuclear data needed by the simulator to a cross section data file in the HDF5 format.
- ANC [27] is the Westinghouse advanced nodal core simulator used for all nuclear core design calculations. The latest version of the ANC code is called ANC9, which introduced a markedly improved pin-power reconstruction methodology [28], that was licensed with the NRC in 2010 [29], which allows for a detailed, node-wise tracking of core depletion parameters and isotopics [30].

These codes are run in the order listed above, with NEXrun controlling the entire cross section generation calculation. The system has been designed to be completely automated. Figure 3-2 summarizes the NEXUS system and the function of each code which compose the system during the cross-section generation process.

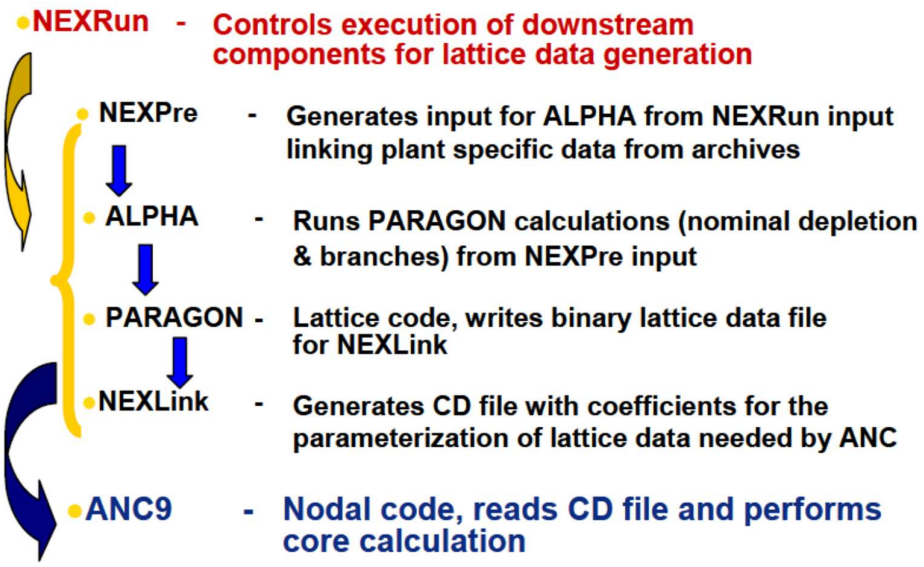

Figure 3-2: Illustration of the NEXUS/ANC9 System [28]

NEXUS includes features needed for the simulation of next generation PWRs. It generates data for the new pin power methodology developed in ANC to capture the effects on pin powers of prolonged control rod insertion. NEXUS also provides the core simulator with the data necessary to deplete control rods.

3.2 PARAGON Lattice Code Methodology

PARAGON is Westinghouse's lattice transport code, written entirely in FORTRAN 90/95. It provides multi-group fuel assembly data for the three-dimensional reactor core calculations done by ANC core simulator. These data include macroscopic cross sections, microscopic cross sections for feedback adjustments, pin factors for pin power reconstruction calculations, and discontinuity factors for a nodal method solution. In addition, it can be used as a standalone code.

PARAGON flux solution is based on collision probability theory with the interface current cell coupling method [31] to solve the integral transport equation. The coupling between adjacent cells is achieved through a discrete angular flux approximation at the cell's surfaces. Throughout the entire calculation, PARAGON uses extract heterogeneous geometry of the assembly and the same energy groups as in the cross section library to compute the multi-group fluxes for each microregion location of the assembly.

PARAGON provides flexibility in modeling that was not available in PHOENIX-P including exact cell geometry representation instead of cylinderization, multiple rings and regions within the fuel pin and the moderator cell geometry, and variable cell pitch. The solution method permits flexibility in choosing the quality of the calculation through both increasing the number of regions modeled within the cell and the number of angular current directions tracked at the cell interfaces.

PARAGON library uses ENDF/B-VI as the source of the basic evaluated data files. The actual library has 70 neutron energy groups (and 48 gamma energy groups), which is the same structure used with PHOENIX-P, but PARAGON is designed to work with any number of energy groups that is specified in the library. This library has been generated using NJOY processing code [32]. To account for the resonance self-shielding effect, the group cross-sections are tabulated as a function of both temperature and background scattering cross-section (dilution). All important fission products are explicit in the library.

In order to generate the multi-group data, PARAGON goes through four steps of calculation: resonance self-shielding, flux solution, leakage correction, burnup calculation, and homogenization [25].

3.2.1 Resonance Self-Shielding

PARAGON uses the collision probabilities to solve the slowing-down equation in pin cells with the real heterogeneous geometry. The resonance self-shielding module is based on Dancoff method where the intermediate resonance assumption is used to approximate the flux shape at the resonance energies [33, 34]. The current version of the code uses a new resonance self-shielding method SDDM (Space Dependent Dancoff Method) for the treatment of the resonance cross-sections. SDDM is the generalization to multi-regions of the method used by PHOENIX-P. The non-regularity of the lattice is taken into account using space dependent Dancoff factor corrections. The multi-region capability is essentially needed to support the fuel rod design codes because of the plutonium buildup at the periphery of the rod. SDDM is described in detail in Reference [33].

The correlations in the PARAGON self-shielding calculation assume that the fuel is in the center of the pellet, radially followed by the clad, and then the moderator. When

modeling dual-cooled fuel, which has moderator in the center region of the pellet, PARAGON's self-shielding calculation would drive unrealistic results.

3.2.2 Flux Solution

The flux solution performed by PARAGON is described in Reference [26] as below:

> *"The neutron (or gamma) flux, obtained from the solution of the transport equation, is a function of three variables: energy, space and angle. For the energy variable, PARAGON uses the multi-group method where the flux is integrated over the energy groups. For the spatial variable, the assembly is subdivided into a number of sub-domains or cells and the integral transport equation is solved in the cells using the collision probability method. The cells of the assembly are then coupled together using the interface current technique. At the interface, the solid angle is discretized into a set of cones, where the surface fluxes are assumed to be constant over each angular cone. PARAGON has been written in a general way so that the cell coupling order is limited only by the computer memory. The collision probability method is based on the flat-flux assumption, which will require subdividing the cells into smaller zones. Thus, for each cell in the assembly, the system of equations to be solved is given by the discretized one energy group transport equation."*

The mathematical formulation of the solution is also described in Reference [35]. As mentioned, the flux solver module is based on the interface current formalism using Collision Probability method within the cells. Notations shown below are documented in Reference [31].

The flux at the surfaces is first discretized into a set of cones:

$$[\varphi, \vartheta] \epsilon [0,2\pi] \times [0,\pi] = \bigcup_{\rho} [\varphi_{\rho}, \varphi_{\rho+1}] \times \bigcup_{\nu} [\vartheta_{\nu}, \vartheta_{\nu+1}]$$

where the flux is independent of the angular variables:

$$\Psi_{\pm,\alpha}^{\rho\nu}(\vec{\Omega}) = \frac{1}{\sqrt{A_{\alpha}^{\rho\nu}}} H(\vec{\Omega} \in \Omega_{\rho\nu})$$

where:

$$A_{\alpha}^{\rho\nu} = \frac{1}{\pi}\int_{(4\pi)} \left(\vec{\Omega}\cdot\vec{n}_{\pm,\alpha}\right) H\left(\vec{\Omega}\in\Omega_{\rho\nu}\right) d\vec{\Omega}$$

and $H\left(\vec{\Omega}\in\Omega_{\rho\nu}\right)$ is the Heaviside distribution defined by:

$$H\left(\vec{\Omega}\in\Omega_{\rho\nu}\right) = \begin{cases} 1 \text{ if } \vec{\Omega}\in\Omega_{\rho\nu} \;\leftrightarrow\; [\varphi,\vartheta]\epsilon\left[\varphi_{\rho},\varphi_{\rho+1}\right]\times[\vartheta_{\nu},\vartheta_{\nu+1}] \\ 0 \text{ if } \vec{\Omega}\notin\Omega_{\rho\nu} \end{cases}$$

The final equation system is given below.

$$\phi_i = \sum_{\alpha,\rho\nu} P_{is_{\alpha}}^{\rho\nu} J_{-,\alpha}^{\rho\nu} + \sum_{j} V_j P_{ij} F_j$$

$$J_{+,\alpha}^{\rho\nu} = \sum_{\beta,\eta\mu} P_{s_{\alpha}s_{\beta}}^{\rho\nu\ \eta\mu} J_{-,\beta}^{\eta\mu} + \sum_{i} P_{s_{\alpha}i}^{\rho} F_i$$

$$J_{-,\alpha}^{\rho\nu} = \sum_{\beta,\eta\mu} B_{\alpha\beta}^{\rho\nu\ \eta\mu} J_{+,\beta}^{\eta\mu}$$

Using the Successive Over Relaxation (SOR) method, this system is solved in PARAGON by iterating on currents and flux. Repetition of unnecessary computation of collision probability matrices is avoided by the usage of transformation laws in order to enhance the code's performance.

3.2.3 Homogenization

The next step in PARAGON calculation after the flux solution is the leakage correction. The leakage correction module uses the same method as in PHOENIX-P. The purpose of this module is to compute the multi-group diffusion coefficients and the multi-group critical flux (spectrum) for the entire homogenized assembly (or parts of the assembly, like baffle/reflector regions). This is usually achieved by solving the fundamental mode of the transport equation [34].

The flux solution to the transport equation is assumed to be separable in a space part and an energy and angle part. It uses B_1 theory to compute the multi-group diffusion coefficients and the multi-group critical spectrum flux used later in other PARAGON

modules. PARAGON uses the number of energy groups in the library to perform these calculations.

Another model to compute the critical flux has been implemented in PARAGON. In this model the neutron source in each micro-region of the assembly is modified by adding a negative absorption proportioned to D_gB^2 [36, 37]. In this case, the diffusion coefficients are first computed using the previous model.

In case of fuel assemblies, the two models are equivalent. The second model is mainly used in the case of critical experiments for which a measured buckling is usually available.

3.2.4 Burnup Calculation

The assembly composition changes following neutron irradiation are obtained by calculating the isotopic depletion and buildup in the heterogeneous geometry, using an effective one-group collapsed flux and cross-sections.

PARAGON depletion module uses the Laplace transform method to solve the set of differential equations after linearizing the isotopic depletion chains. This module is general and any new chain can be added easily without any changes in the code. In addition, it uses the predictor/corrector technique to better account for the flux level variation [34].

It is capable of depleting the detailed micro-regions specified in the user input [33]. The code detects automatically the regions to be depleted, but the user has the option to hold any region in the assembly as non-depletable. For boron depletion, the user has a choice on depleting it according to a letdown curve that is provided through the input or exponentially (i.e., depletion chain).

3.2.5 Other Modeling Capabilities

PARAGON has a module that interpolates in the temperature tables to compute the temperatures for each isotope present in the model before calling the self-shielding module for cross-sections calculations.

A Doppler branch calculation capability is built into PARAGON. This capability permits fuel temperature variations to be modeled while keeping all other parameters

constant. Results of these calculations are used to generate changes in some parameters which are passed to the core models to capture Doppler effects.

A model to expand the radii of the cylindrical region has been implemented in PARAGON. The code uses this capability mainly in the case of the Doppler branch calculation. It also has a flag to turn it on in any calculation step.

PARAGON has the flexibility of printing many types of micro and macro physics parameters. Hence the user can request to edit the fluxes, partial currents, surface fluxes, different reaction rates, isotopic distribution etc. The editing could be done for micro-regions, or as an average over a cell or as an average over a group of cells, and for any number of energy groups (i.e. the code can collapse to any number of groups for editing).

Finally, PARAGON is also able to model reflectors and generate the reflector constants.

3.3 PARAGON Qualification

The qualification of a nuclear design code is a large undertaking since it must address the qualification of the methodology used in the code, the implementation of that methodology, and its application within a nuclear design system. For this reason, Westinghouse has historically used a systematic qualification process which starts with the qualification of the basic methodology used in the code and proceeds through logical steps to the qualification of the code as used with an entire nuclear design code system [35].

PARAGON was qualified in 2003 and its qualification is documented in WCAP-16045 [26]. This qualification followed the same process used when qualifying the PHOENIX-P/ANC system [38].

This qualification process is composed of three parts:

1. Comparison of standalone PARAGON to several critical experiments and isotopic measurements.
2. Comparisons of assembly calculations to the Monte Carlo code MCNP for a variety of PWR assembly lattice types, burnable absorbers, a large enrichment range and both U02 and MOX. Both continuous as well as

multi-group options of MCNP have been used. PARAGON was also compared against its predecessor, PHOENIX-P. Results are shown for both reactivity and power distribution.

3. Comparisons against measured plant data. A large type of PWR plants have been used ranging from standard Westinghouse plants (14x14, 15x15, 16x16 and 17x17 assembly fuel types) to CE (Combustion Engineering) to MOX fuel plants to MHI (Mitsubishi Heavy Industries) plants. This has permitted to test all capabilities of PARAGON, like the treatment of burnable absorbers (Gadolinium, Erbium, IFBA, etc), the control rod worth, etc. Startup test results, critical boron versus burnup and radial power distributions were compared. In addition, PARAGON/ANC results were compared against PHOENIX-P/ANC.

The first two parts qualify the methodology used in the code and its implementation. The third part qualify the use of the code for core design applications.

The large variety in the cycles chosen for this qualification serves to demonstrate the robustness of PARAGON and its library to analyze over a large range of cycle designs; and it serves to qualify PARAGON to analyze each feature by direct comparison of results.

3.4 PARAGON2

PARAGON2 is the new Westinghouse neutron and photon transport lattice code which is currently being reviewed by NRC. PARAGON2 was developed following first principle physics models, avoiding weak approximations in the solution algorithms of the transport equation. The goal of using this strategy is to improve the predictions in the current plants, while allowing the code to be used for any fuel assembly type, regardless of the complexity of the geometry design and composition.

The main new improvements incorporated in PARAGON2 are summarized as follows [39, 40]:

PARAGON2 employs Ultra-Fine Energy Mesh Library (UFEML) with 6064 neutron and 97 gamma energy groups for multi-group cross section calculations. The library is based on ENDF/B-VII.1 (and JEFF3.2) and will eventually contain all the

isotopes available in the ENDF/B-VII.1 basic nuclear data repository. This new library has been extensively benchmarked against Monte Carlo continuous energy solution for all types of fuel assemblies, currently in use, and against critical experiments. In addition, no adjustment is needed for the cross-sections of this library to be used; they are processed through NJOY [41] code and are used, as they are, from the source.

- All the scattering matrices of the isotopes in UFEML are based on the anisotropic Resonance Scattering Model (RSM) described in Ref. [42], except for hydrogen in water and the graphite as addressed in Ref. [42]. The effect of this improvement is that the resonance self-shielding calculation is eliminated [40], which is expected to allow the code to better model non-standard fuel types, such as the dual-cooled fuel. The modeling becomes geometrically independent, as the equivalence relations used in the self-shielding calculations are usually formulated for solid cylindrical rods, where the material in the center of the rod is fuel and not water.
- The depletion chains in PARAGON2 have been extended to track 116 fission products and 25 actinides. In the point of view of the memory management and the running time performance of the code, these detailed depletion chains are a challenging problem for UFEML method. The energy dependent fission products yields were also implemented in PARAGON2, if available within ENDF/B-VII.1.
- All the modules in the code that necessitate the multigroup energy formulation use the 6064 groups without any collapse inside the code. This approach requires sophisticated programing algorithms for better memory management.

The collision probability and interface current methods were used in the flux solution as described in Ref. [36].

The main disadvantage of PARAGON2 is that it is much more computationally intensive than the standard PARAGON, due to the advanced methods it uses. To balance this, parallel computing algorithms were introduced throughout the code using the shared-memory multi-core processing OpenMP directives [39].

PARAGON2's topical report was submitted to NRC in October 2019 [56]. In addition to the description of the new physics models implemented, this report contains a validation of PARAGON2 with Monte Carlo method. For this validation, numerical assembly benchmarks were made covering all PWR fuel types, including 14x14, 15x15, 16x16, 17x17 Westinghouse and CE assemblies with OFA and RFA fuel and IFBA, Gad, and Erbia burnable absorbers [40]. In addition, Critical Experiments and PIE (Post Irradiation Experiments) were evaluated using PARAGON2. Finally, plant data analysis using the NEXUS system with PARAGON2 were done, for all Westinghouse and CE 2-, 3-, and 4-loop core types, covering HZP, HFP conditions and typical safety analysis.

An input for PARAGON2 is exemplified in Appendix A.

4 MCNP6 Code

The current section focusses on the MCNP6 code, which was used to create the benchmarks to be compared against PARAGON2 results. While Section 4.1 describes the MCNP methodology, Section 3.2 focuses on the usage of MCNP results for code validation.

4.1 Methodology

Monte Carlo is a method of statistical simulation that uses a sequence of random numbers to simulate physical systems, which is particularly interesting in the resolution of problems to which deterministic methods are not suitable. In the Monte Carlo method, individual probabilistic events which compose a system are modeled sequentially [43].

Among many applications, the Monte Carlo method has been applied to the particle transport to reproduce statistical processes of atomic and nuclear iteration. For that, each of the many primary and secondary particles are generated, starting from a radioactive source in a system. The codes that do this simulate computationally particle emission and detection, employing random numbers to determinate the location where particles were generated and their emission direction. These codes compute all events, such as radiation absorption, Compton scattering, Bremsstrahlung radiation, X-ray production, among others, and report the results with their respective statistical error. In other words, each of many particles produced by an emission source is tracked from its creation until its final threshold energy, and between that its iterations are stablished randomly. Figure 4-1 illustrates the random history, with its many iterations, of a neutron incident on a slab of fissionable material [44].

The Monte Carlo N-Particle (MCNP) is the internationally recognized code for analyzing the transport of neutrons and gamma rays (hence NP for neutral particle) by applying this methodology. This code is developed and maintained by the Los Alamos National Laboratory (LANL) [45]. It is a “general-purpose, continuous-energy, generalized-geometry, time-dependent”, Monte Carlo code with a wide range of applications.

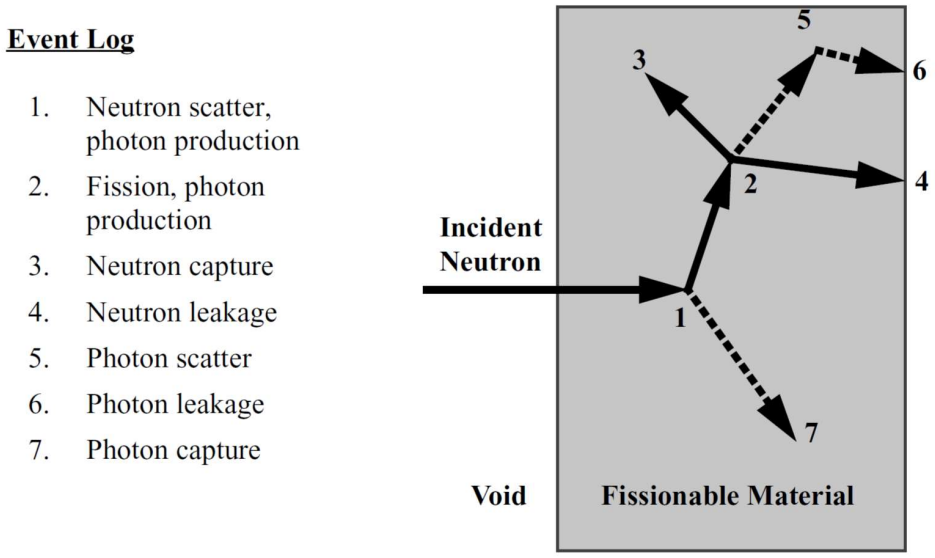

Figure 4-1: Illustration of a random neutron history [44]

The Monte Carlo simulations used by MCNP vary significantly from those of the deterministic methods, such as the ones mentioned in Section 3. In this case, statistical processes (such as nuclear particles interacting with matter) can be theoretically reproduced using random number generators. The probability distribution functions of these processes are determined and the cross sections for each possible event, as specified by user defined data libraries, as well as the conditions of the problem are taken into account. These functions can then be sampled, tallied, and statistically analyzed to describe the entire phenomenon of interest [46].

While deterministic methods typically give fairly complete information throughout the phase space of the problem, MCNP provides information only about the specific tallies that are requested by the user, along with the estimates of the statistical precision (uncertainty) of these results [44].

MCNP is found to be particularly useful for complex, three-dimensional, time-dependent simulations in which many deterministic approaches cannot accurately describe the conditions or geometry. This suitability is due to the fact that it does not use phase space boxes and therefore no averaging approximations are required in space, energy, and time.

MCNP6 is one of the latest versions of MCNP. It was released in 2013 while merging the capabilities of the two current versions at that time (MCNP5 and MCNPX)

[47]. This version is able to model the transport of 37 particle types, ranging from elementary particles, composite particles and composite antiparticles, and nuclei. In addition to that, more than 25 new features (not found in either code) were implemented, such as the A adjoint-based sensitivity coefficients, the geometry mesh file creation, the capability to track and tally neutrons and photons on an unstructured mesh geometry and new depletion capabilities. The new features are further detailed in References [48] and [47].

An input for MCNP6 is exemplified in Appendix B. More information on the input structure can be found in References [45] and [48].

4.2 Usage for Code Validation

Numerical transport simulation has become more and more attractive for the benchmarking of radiation transport modeling codes with the increasing experimental costs and decreasing computational costs. As described in Reference [49]:

"*The transport numerical models […] are of great value to code validation for the following reasons: they verify that the code functions properly; they verify that the cross-section data used by the code are accurate; and they hep certify that a user has learned to use the code correctly."*

Due to its versatility in modeling complex problems and the well-known accuracy, MCNP has been extensively used in the nuclear industry for code-to-code benchmarking. For instance, Reference [35] and [26] documents how the code was used for the NRC qualification process of PARAGON for PWR core applications, as also described also in Section 3.2. In Reference [50], the numerical validation of the lattice physics capability available in the code MPACT is done by comparison against MNCP5 and other codes. As seen in Reference [51], even SERPENT, which is another Monte Carlo code, was extensively validated by comparing to MCNP results.

5 Proposed Models

The current section discusses the proposed models for determination of the effects of dual-cooling on annular fuel neutronic calculations. Section 5.1 covers the cross-section library used. Section 5.2 describes the geometrical and material information of the models. Section 5.3 discusses the assumed temperature information. Section 5.4 briefly describes the modeling difference between using PARAGON2 and MCNP. Section 5.5 covers the parameters of interest that were analyzed, and Section 5.6 explains the assumed acceptance criteria.

In all MCNP calculations, 50,000 neutrons per cycle were modeled.

5.1 Cross-Section Library

Evaluated nuclear data are needed by simulation codes in order to perform neutronic calculations. The ENDF (Evaluated Nuclear Data Files) formats and libraries are one of the most used options to encode nuclear data evaluations for use in research and nuclear technology. They are decided by the Cross-Section Evaluation Working Group (CSEWG), which is a cooperative effort of industry, national laboratories, and universities in the United States and Canada, and are maintained by the National Nuclear Data Center (NNDC) [52].

As described in Reference [53], "ENDF-format libraries are computer-readable files of nuclear data that describe nuclear reaction cross sections, the distributions in energy and angle of reaction products, the various nuclei produced during nuclear reactions, the decay modes and product spectra resulting from the decay of radioactive nuclei, and the estimated errors in these quantities".

Both PARAGON2 and MCNP calculations were performed using a cross-section library based on the ENDF/B-VII.1 evaluated nuclear reaction data library. MCNP6 was released packaged with nuclear data files usable by MCNP based on this version of the library. This data consists of 423 nuclides processed to 7 temperatures suitable for reactor simulations [47]. All of the changes implemented in this version of the library are detailed in Ref. [54] and the rest of the December 2011 issue of Nuclear Data Sheets. Having the

same Evaluated nuclear data as a basis for the cross-section libraries for both codes ensures more comparability between the results.

5.2 Fuel models

Using both a pin cell model and an assembly model, PARAGON2 was benchmarked against MCNP for a typical PWR solid fuel design and two annular fuel designs.

Reference [4] proposed two annular fuel designs labeled as PQN-01 (15x15 lattice) and PQN-02 (13x13 lattice). When proposing these, the overall assembly size was kept the same as the typical Westinghouse PWR 17x17 lattice assembly. Following this Reference, these two annular fuel models were modeled as well as the standard solid 17x17. Table 5-1 gives the geometric dimensions of these three fuel lattices.

Table 5-1: Geometric data for analyzed fuel lattices (in units of cm) [4]

Cases	Solid Fuel (17x17)	Annular Fuel PQN-01 (15x15)	Annular Fuel PQN-02 (13x13)
Pin pitch	1.26	1.431	1.651
Rod inner radius	-	0.3365	0.4315
Inner clad outer radius	-	0.3935	0.4890
Fuel inner radius	-	0.4000	0.4950
Fuel outer radius	0.4096	0.5990	0.7050
Outer clad inner radius	0.4178	0.6050	0.7110
Rod outer radius	0.4750	0.6600	0.7685

These geometries were used to model both pin cell models and assembly models in PARAGON2 and MCNP using the same material compositions and geometrical configurations. The gaps were explicitly modeled, following the radii given in Table 5-1.

In all cases, the fuel is UO_2 at 4.95 enrichment and 95% theoretical density.

In order to see the effects of absorption in the central region of the annular fuel, the water was modeled not only with no Boron but also with 500 ppm of Boron.

5.3 Temperature information

Since the MCNP cross-sections were available only at 600 and 900 K, the temperatures in PARAGON2 were modeled accordingly.

With that, the calculations were done at typical HZP and HFP temperature conditions, as below:

- HZP: both fuel and coolant were modeled at 600 K.
- HFP: fuel is modeled at 900 K and coolant is modeled at 600 K.

These temperature conditions were applied to both the pin cell and the assembly models. In addition, a flat fuel temperature profile was assumed in the fuel, given the availability of cross-sections only at the aforementioned temperatures.

5.4 Modeling Differences

When modeling the gaps, MCNP is able to model it as void (composition 0). However, in PARAGON, that option is not available. Therefore, the gap was modeled as a region with Al (material 13027) at a very low density (1.000000E-06 nuclei/cc).

5.5 Parameters of interest

When analyzing the results from both the MCNP and PARAGON2 models, several neutronic quantities of interest were calculated.

For the pin cell models, the eigenvalues (K_∞) obtained in the two codes were compared, for all cases. An agreement between the two shows that PARAGON2 is able to predict the reactivity in the dual-cooled fuel. In addition, the conversion ratio (C*) was also calculated. This quantity is given as the ratio of U-238 capture rate to U-235 fission rate and an agreement indicates that the physical reactions are being modeled accurately. Finally, the radial power distribution within the pin was calculated, assuming a flat temperature profile, as described in Section 5.2. For calculating the radial power distribution, the fuel part of the pin cells was divided into 10 equal volume rings. This parameter is important to show that impacts of cooling and moderation in the center region of the dual-cooled annular fuel are captured correctly by the models.

For the assembly models, the eigenvalues were compared, as done for the pin models. In addition, the pin power distribution in the assembly was calculated. The power distribution is important as not only the peak pin power is the basis of many safety parameters, but also it is used for the pin power reconstruction in the core simulator (ANC).

Furthermore, using the depletion module in PARAGON, the assemblies with Boron in the moderator were depleted until 82,000 MWD/MTU in order to compare how the multiplication factor changes with burnup for the solid and annular fuel assemblies. No depletion was performed in MCNP, as PARAGON depletion includes the energy released from neutron capture besides the fission energy release and MCNP depletion module does not cover that.

5.6 Acceptance Criteria

Two approaches were taken for judging whether PARAGON2 results would be acceptable when compared to MCNP results for modeling dual-cooled annular fuel. This was done in order to help indicate the acceptance criteria for the parameters of interest of this study.

Firstly, both pin cell and assembly models were created not only for dual-cooled fuel but also for standard solid 17x17 fuel. An expectation is that the difference between PARAGON2 and MCNP results for the dual-cooled fuel would be at the same level of magnitude as the difference seen for the standard solid fuel. This would indicate that PARAGON2 is able to model dual-cooled fuel with the same accuracy it is able to model standard solid fuel.

In addition, a review of past benchmarks in literature was done to establish what results were deemed acceptable in similar analysis. Table 5-2 lists the maximum absolute differences that were observed.

Table 5-2: Summary of Maximum absolute differences observed in Literature

Reference	Pin Cell Model		Assembly Model	
	K_∞ (pcm)	**Conversion Ratio (%)**	**K_∞ (pcm)**	**Pin Power Distribution (%)**

4 (DCF – CASMO-4 vs. MCNP-4C)	-	9.09	2965	-
22 (DCF in SCWR – FENNEL-4 vs. MCNP)	-	-	687	8.37
4 (Solid – CASMO-4 vs. MCNP-4C)	-	-	346	-
35 (Solid, PARAGON vs. MCNP)	-	-	163	1.71
33 (Solid, PARAGON vs. MCNP)	164	-	-	-
39 (Solid, PARAGON2 vs. SERPENT2)	79	-	231	2.10

With these two approaches, it was concluded that maximum eigenvalue differences below 350 pcm and pin power distributions differences below 2.5% would be acceptable. In addition, a difference in conversion ration below 9% would represent an improvement from past analysis.

6 Results

6.1 Pin Cell Results

Following the modelling described in Section 5, pin cells were modeled for the three fuel geometries in both PARAGON2 and MCNP. The neutronics resulted from using the two codes are compared in the following subsections.

6.1.1 K_∞ Comparison

Table 6-1 shows a comparison of the pin cell model eigenvalues from PARAGON2 and MCNP, for both the standard solid fuel and the annular fuel. As can be seen, the solid fuel reactivity differences are smaller than the annular fuel ones, which are around -200pcm.

In general, it can be seen that the annular fuel has lower eigenvalues than the solid fuel. This behavior is expected given that the annular fuel pin is cooled from both sides, which increase the resonance capture, reducing then the eigenvalue.

Table 6-1: Comparison of PARAGON2 and MCNP Eigenvalues for Pin Models

Cell Type	Power	Boron (ppm)	k_∞		$\Delta k\infty$ (pcm)
			PARAGON2	MCNP	PARAGON2-MCNP
Solid Fuel (17x17)	HFP	0	1.40307	1.40485	-126.78
	HZP		1.41444	1.41603	-112.35
PQN-01 (15×15)	HFP		1.34775	1.35074	-221.61
	HZP		1.36195	1.36466	-198.78
PQN-02 (13×13)	HFP		1.37061	1.37384	-235.38
	HZP		1.38438	1.38718	-202.05
Solid Fuel (17x17)	HFP	500	1.35770	1.35900	-95.70
	HZP		1.36865	1.37007	-103.70
PQN-01 (15×15)	HFP		1.30748	1.31021	-208.58
	HZP		1.32117	1.32342	-170.16
PQN-02 (13×13)	HFP		1.32454	1.32696	-182.54
	HZP		1.33777	1.33980	-151.63

6.1.2 Radial Power Distribution

Figures Figure 6-2 and Figure 6-2 are comparisons of PARAGON2 and MCNP radial power distributions for the solid fuel (17x17) pin cell model. The maximum difference between the two codes for this model was 0.06%.

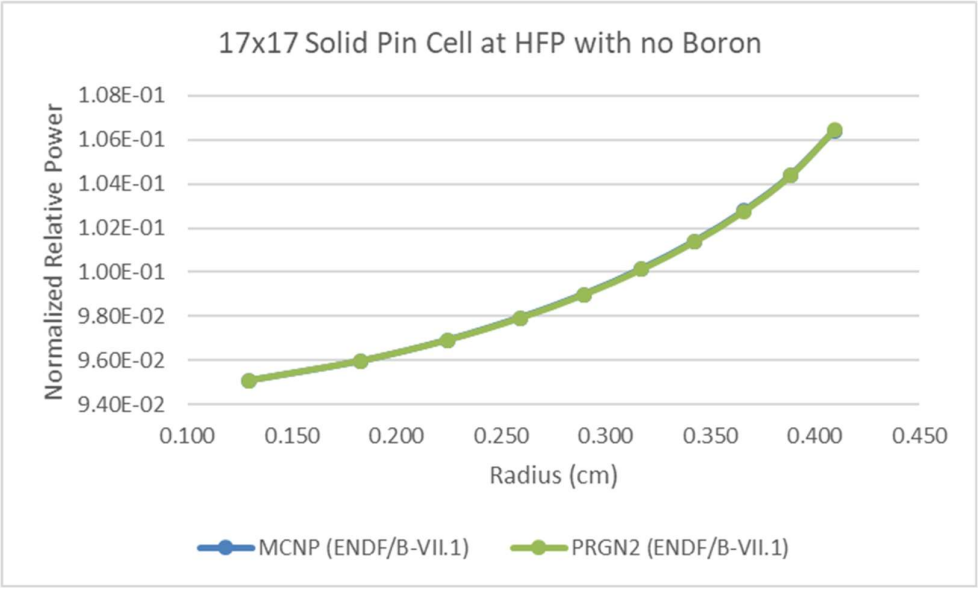

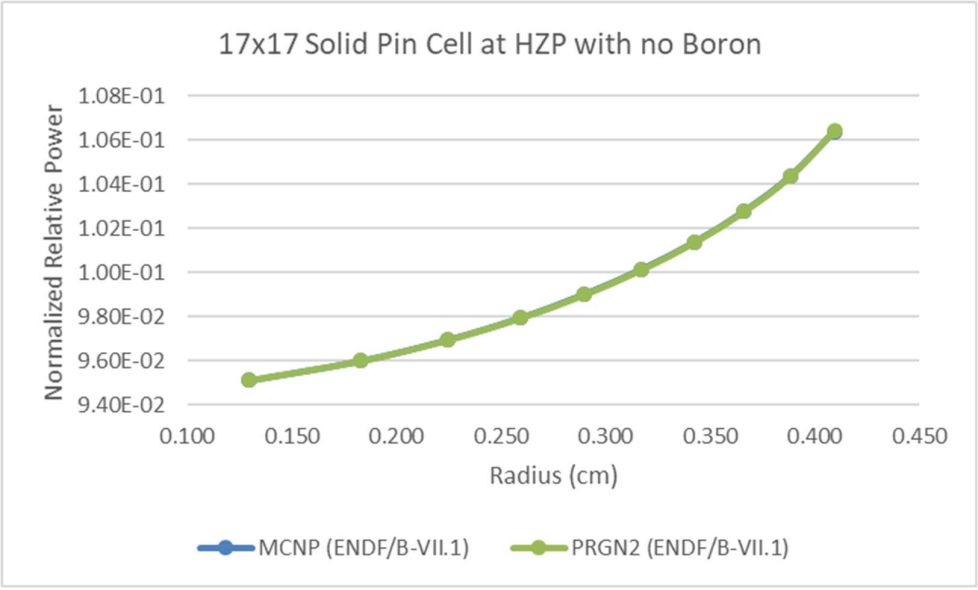

Figure 6-1: Comparison of PARAGON2 and MCNP Radial Power Distributions for Solid (17x17) Pin Cell with no Boron

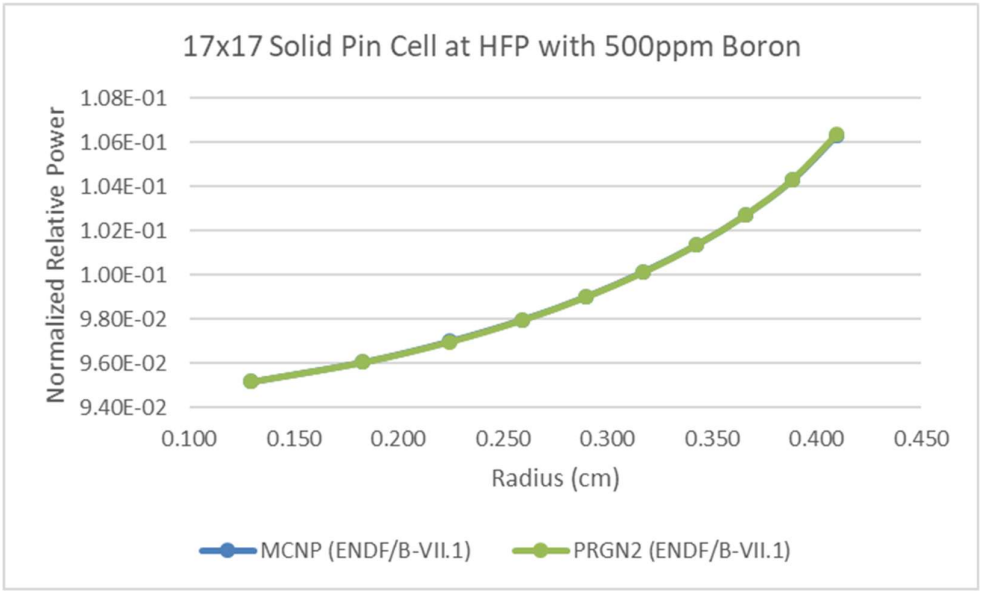

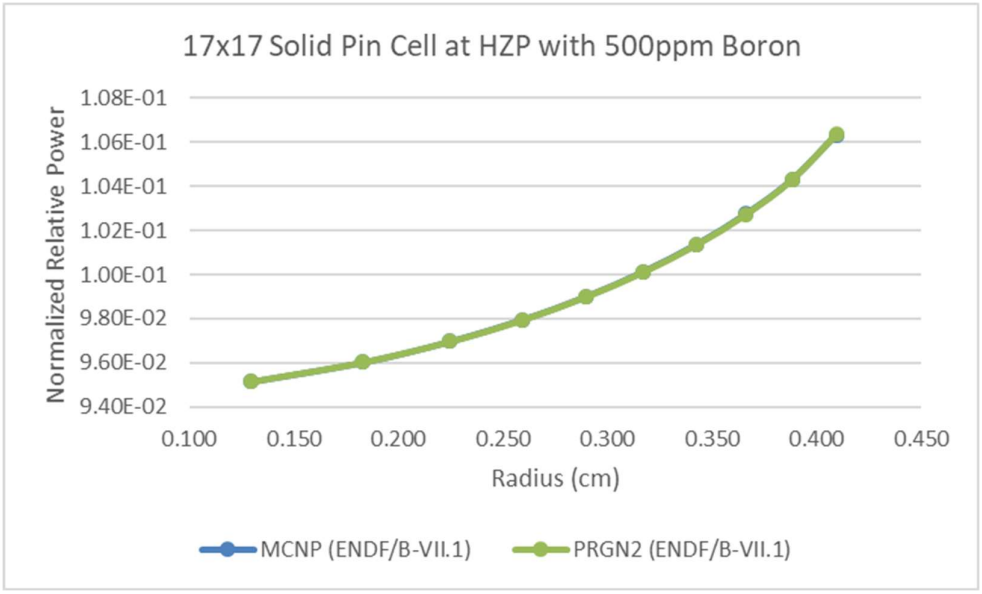

Figure 6-2: Comparison of PARAGON2 and MCNP Radial Power Distributions for Solid (17x17) Pin Cell with 500 ppm Boron

Figure 6-3 and Figure 6-4 are comparisons of PARAGON2 and MCNP radial power distributions for the PQN-01 (15x15) pin cell model. The maximum difference between the two codes for this model was 0.08%.

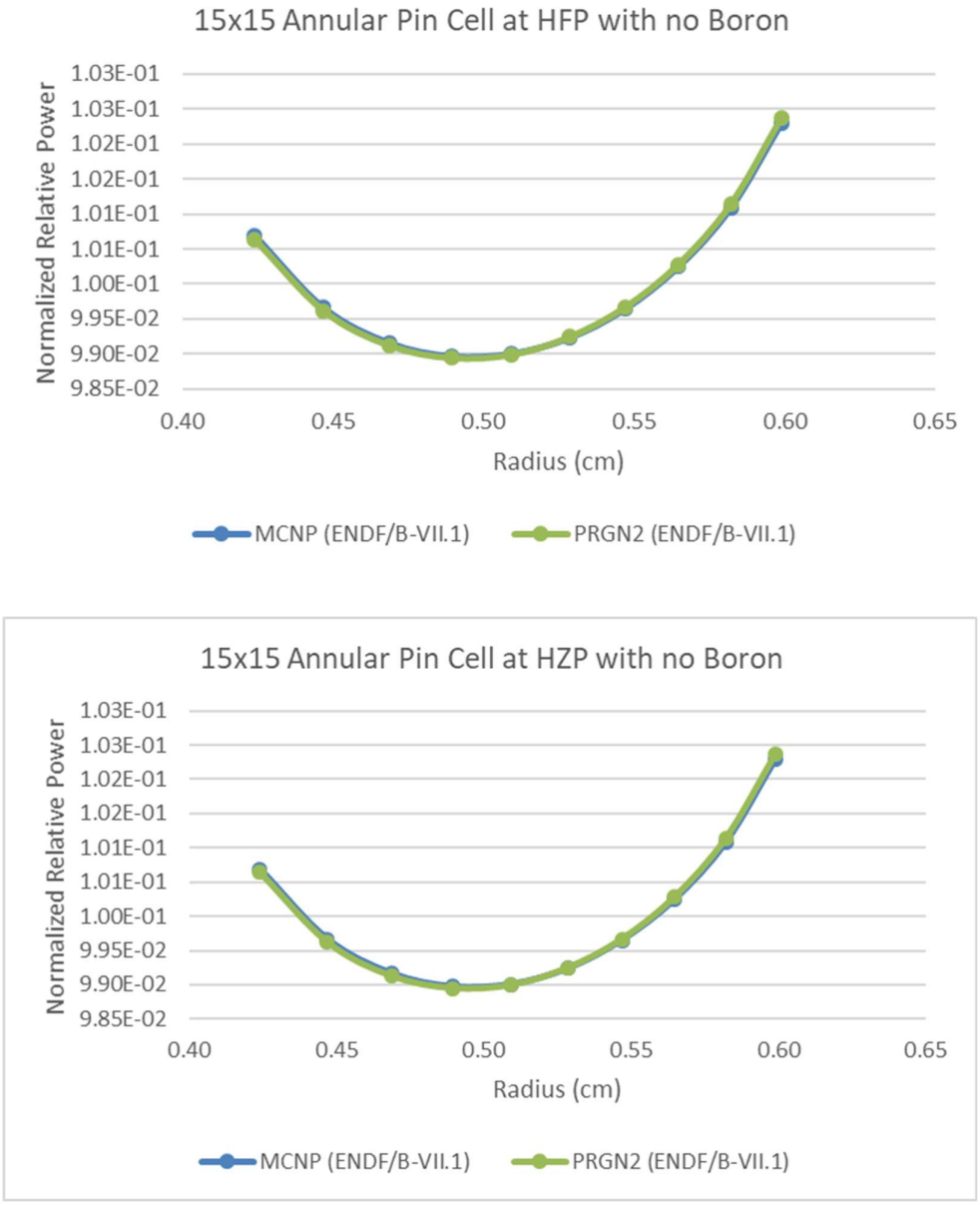

Figure 6-3: Comparison of PARAGON2 and MCNP Radial Power Distributions for PQN-01 (15x15) Pin Cell with no Boron

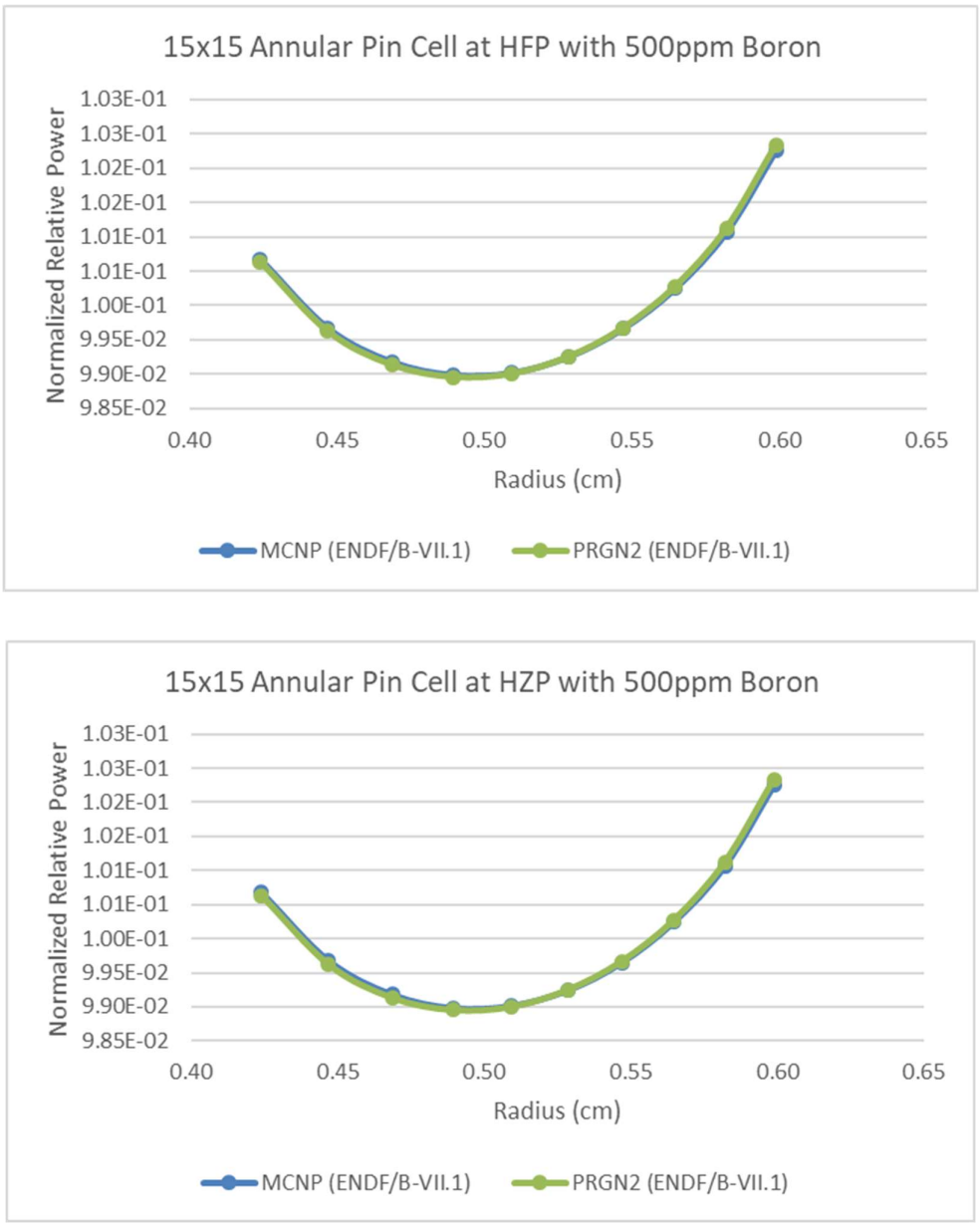

Figure 6-4: Comparison of PARAGON2 and MCNP Radial Power Distributions for PQN-01 (15x15) Pin Cell with 500 ppm Boron

Figure 6-5 and Figure 6-6 are comparisons of PARAGON2 and MCNP radial power distributions for the PQN-02 (13x13) pin cell model. The maximum difference between the two codes for this model was 0.10%.

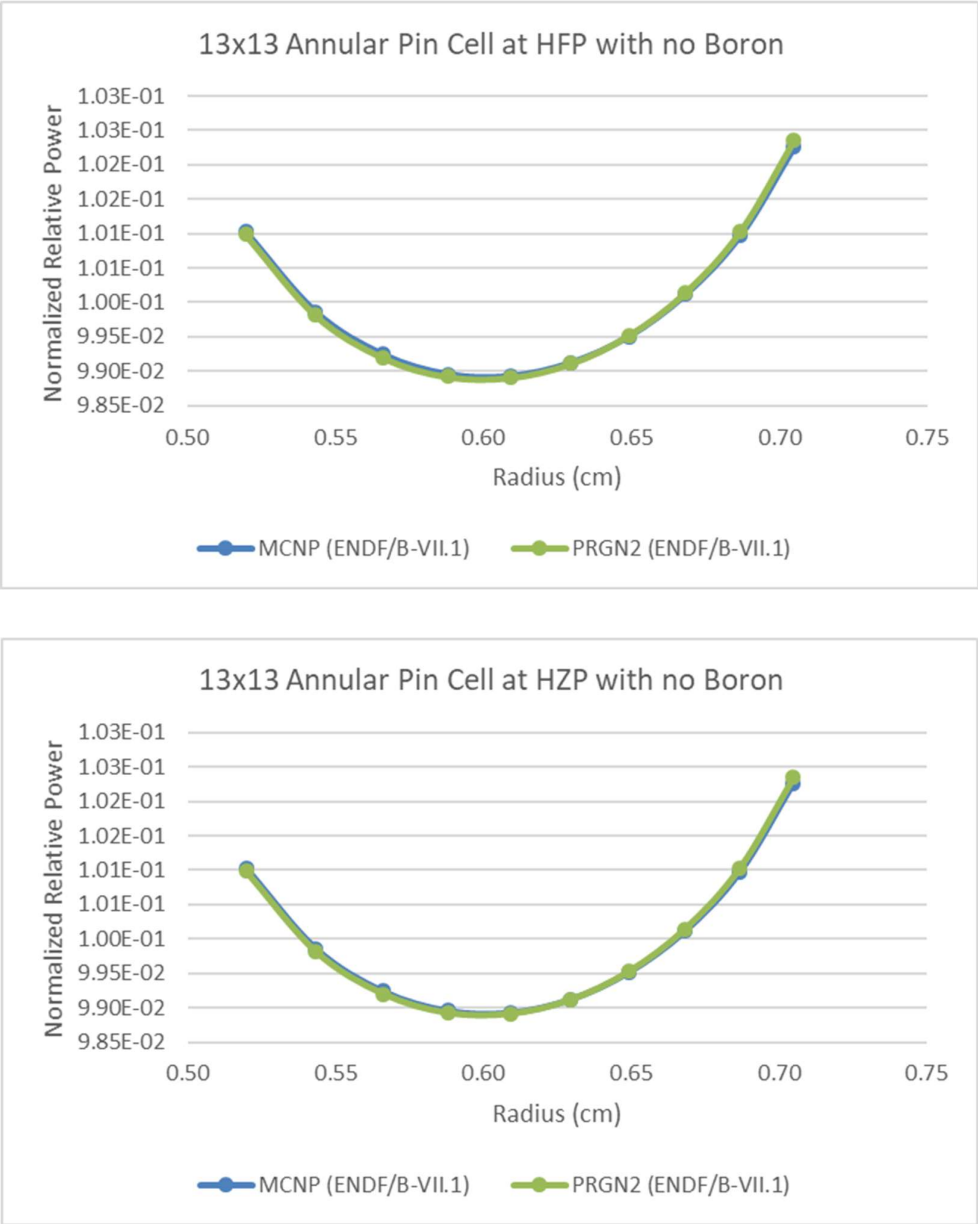

Figure 6-5: Comparison of PARAGON2 and MCNP Radial Power Distributions for PQN-02 (13x13) Pin Cell with no Boron

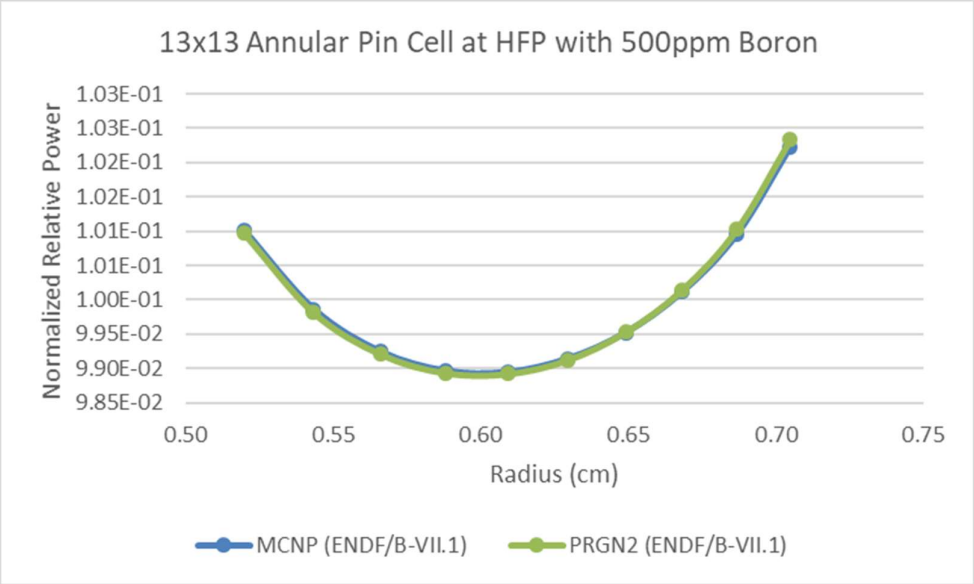

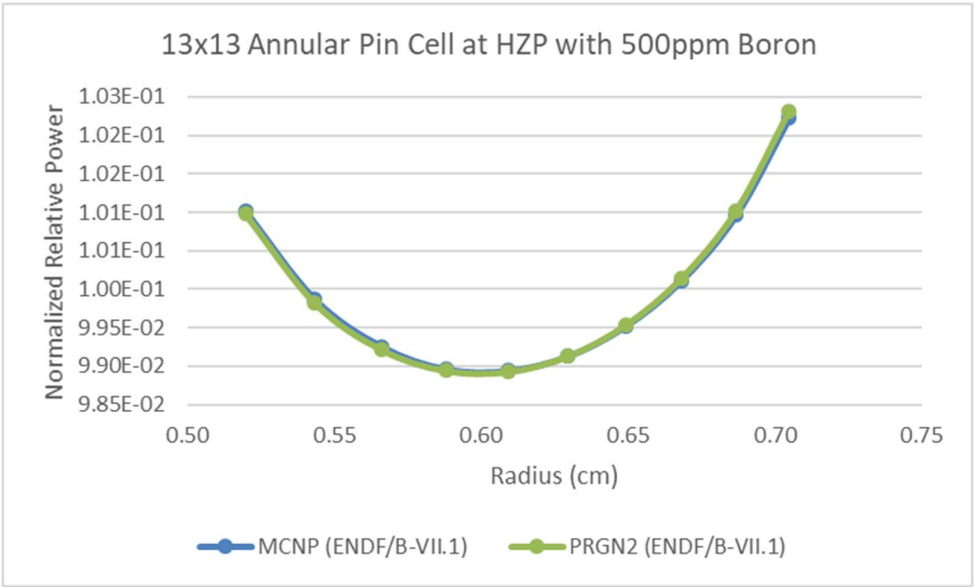

Figure 6-6: Comparison of PARAGON2 and MCNP Radial Power Distributions for PQN-02 (13x13) Pin Cell with 500 ppm Boron

As can be seen, both annular models had radial power differences of the same magnitude as the solid model one. This indicates that PARAGON2 can radially model the annular fuel with a similar accuracy as with the solid fuel. It is also worth noticing that in the annular fuel there is no major discrepancy in the predictions in the radial extremes of the fuel, which is the area most affected by the resonance self-shielding. This proves PARAGON2's geometrically-independent capability.

In addition, one can notice that the power gradient in the annular fuel is much smaller than that of the solid fuel. This is expected given that the DCF has moderation in its inner region, as it has fuel surfaces cooled from both sides.

6.1.3 Conversion Ratio

Table 6-2 compares the Conversion Ratio (C*) from the pin cells modeled in PARAGON2 and MCNP. As can be seen, PARAGON2 was able to predict the Conversion Ratio with a similar level of accuracy for both the solid pins and the annular pins.

In addition, it can be noticed that in general the annular fuel has a higher conversion ratio than the solid fuel. This behavior is explained by the additional U-238 capture from the water presence inside of the annular fuel, which drives for a higher U-238 capture rate (the numerator of the conversion ratio). The same logic is valid for the cases with and without Boron in the moderator.

Table 6-2: Comparison of PARAGON2 and MCNP Conversion Ratios for Pin Models

Cell Type	Power	Boron (ppm)	C* (Conversion Ratio)		ΔC* (%)
			PARAGON2	MCNP	PARAGON2-MCNP
Solid Fuel (17x17)	HFP	0	0.4980	0.4805	3.64%
	HZP		0.4825	0.4660	3.53%
PQN-01 (15×15)	HFP		0.5595	0.5418	3.25%
	HZP		0.5391	0.5223	3.21%
PQN-02 (13×13)	HFP		0.5254	0.5074	3.55%
	HZP		0.5063	0.4893	3.48%
Solid Fuel (17x17)	HFP	500	0.5101	0.4942	3.23%
	HZP		0.4941	0.4787	3.21%
PQN-01 (15×15)	HFP		0.5724	0.5560	2.96%
	HZP		0.5515	0.5360	2.88%
PQN-02 (13×13)	HFP		0.5389	0.5224	3.14%
	HZP		0.5192	0.5038	3.06%

6.2 Assembly Results

Following the modelling described in Section 5, fuel assembly lattices were modeled for the three fuel geometries in both PARAGON2 and MCNP. The neutronics resulted from using the two codes are compared in the following subsections.

6.2.1 K_∞ Comparison

Table 6-3 shows a comparison of the assembly model eigenvalues from PARAGON2 and MCNP, for both the standard solid fuel and the annular fuel. On the contrary of the pin models, for the assembly models the solid fuel reactivity differences are slightly larger than the annular fuel ones. All of them being below 250pcm of

magnitude. The results in this table show that PARAGON2 predicts with a very high accuracy the Monte Carlo results.

Table 6-3 - Comparison of PARAGON2 and MCNP Eigenvalues for Assembly Models

Assembly Type	Power	Boron (ppm)	k∞		Δk∞ (pcm)
			PARAGON 2	MCNP	PARAGON2-MCNP
Solid Fuel (17x17)	HFP	0	1.43325	1.43627	-210.49
	HZP		1.44397	1.44666	-186.12
PQN-01 (15×15)	HFP		1.38965	1.39250	-204.88
	HZP		1.40276	1.40523	-175.93
PQN-02 (13×13)	HFP		1.39530	1.39836	-219.07
	HZP		1.40837	1.41108	-192.24
Solid Fuel (17x17)	HFP	500	1.37711	1.37966	-185.00
	HZP		1.38734	1.38961	-163.49
PQN-01 (15×15)	HFP		1.33713	1.33940	-169.62
	HZP		1.34969	1.35145	-130.32
PQN-02 (13×13)	HFP		1.34110	1.34348	-177.31
	HZP		1.35360	1.35546	-137.32

6.2.2 Pin Power Distribution

Figure 6-7 is a comparison of PARAGON2 and MCNP assembly pin power distributions for the solid fuel (17x17) assembly model. The maximum difference between the two codes for this model was 0.70%.

17x17 Solid Pin Cell at HFP with no Boron

0.16%								
-0.17%	-0.39%							
-0.22%	-0.41%	-0.10%						
-0.29%	-0.28%	-0.22%						
-0.19%	-0.15%	0.30%	0.69%	0.47%				
0.10%	-0.04%		0.24%	0.09%				
-0.11%	0.06%	-0.10%	0.18%	0.25%	0.13%	-0.02%		
-0.24%	0.05%	-0.12%	0.25%	0.10%	-0.10%	0.11%	0.11%	
0.04%	-0.10%		-0.02%	-0.07%		0.00%	-0.16%	

17x17 Solid Pin Cell at HFP with 500ppm Boron

0.32%								
-0.29%	-0.62%							
-0.20%	-0.40%	0.23%						
-0.22%	-0.29%	-0.03%						
0.05%	0.13%	0.35%	0.51%	0.60%				
-0.07%	-0.11%		0.10%	0.16%				
-0.34%	-0.02%	-0.09%	-0.04%	0.11%	-0.11%	-0.04%		
-0.25%	0.01%	0.02%	0.15%	0.20%	-0.01%	-0.03%	0.17%	
-0.19%	-0.08%		0.13%	0.00%		0.12%	-0.09%	

17x17 Solid Pin Cell at HZP with no Boron

-0.02%								
-0.42%	-0.70%							
-0.28%	-0.62%	-0.06%						
-0.41%	-0.42%	0.06%						
-0.19%	-0.15%	0.55%	0.44%	0.57%				
-0.13%	-0.15%		0.25%	0.27%				
-0.07%	-0.14%	-0.09%	0.14%	0.22%	0.08%	0.26%		
-0.22%	0.20%	0.12%	0.14%	0.12%	0.17%	0.09%	0.27%	
-0.02%	-0.14%		-0.19%	-0.04%		0.10%	0.12%	

17x17 Solid Pin Cell at HZP with 500ppm Boron

0.36%								
-0.37%	-0.70%							
-0.33%	-0.33%	-0.10%						
-0.06%	-0.28%	0.25%						
0.16%	0.11%	0.20%	0.42%	0.43%				
-0.12%	-0.25%		0.18%	0.12%				
-0.01%	0.02%	0.21%	0.22%	0.09%	0.01%	-0.19%		
-0.36%	0.08%	0.10%	-0.06%	0.28%	-0.12%	0.07%	-0.05%	
-0.12%	-0.14%		0.01%	0.08%		0.23%	-0.24%	

Figure 6-7: Comparison of PARAGON2 and MCNP Assembly Pin Power Distributions for Solid (17x17) Assembly Model

Figure 6-8 is a comparison of PARAGON2 and MCNP assembly pin power distributions for the PQN-01 (15x15) assembly model. The maximum difference between the two codes for this model was 0.87%.

15x15 Annular Pin Cell at HFP with no Boron

-0.03%							
-0.23%	-0.19%						
-0.33%	-0.09%						
-0.26%	-0.12%	0.31%	0.73%				
-0.20%	-0.19%	0.01%	0.80%				
-0.35%	-0.01%		0.62%	0.18%	-0.17%		
-0.30%	-0.17%	0.58%	0.80%	-0.01%	-0.38%	-0.20%	
-0.29%	-0.43%	0.08%		0.11%	-0.64%	0.00%	

15x15 Annular Pin Cell at HFP with 500ppm Boron

0.11%							
-0.32%	-0.29%						
-0.20%	-0.09%						
-0.16%	-0.01%	0.17%	0.72%				
-0.10%	0.20%	0.03%	0.62%				
-0.18%	0.11%		0.54%	-0.08%	-0.20%		
-0.02%	-0.12%	0.41%	0.64%	-0.17%	-0.37%	-0.05%	
-0.21%	-0.66%	0.05%		0.04%	-0.62%	-0.08%	

15x15 Annular Pin Cell at HZP with no Boron

0.14%							
-0.06%	-0.42%						
-0.32%	-0.32%						
-0.19%	0.09%	0.11%	0.67%				
-0.22%	-0.03%	0.10%	0.65%				
-0.35%	-0.10%		0.62%	0.18%	-0.22%		
-0.22%	-0.18%	0.67%	0.87%	0.07%	-0.42%	-0.02%	
-0.48%	-0.66%	0.14%		0.21%	-0.60%	-0.08%	

15x15 Annular Pin Cell at HZP with 500ppm Boron

0.16%							
-0.17%	-0.23%						
-0.49%	-0.05%						
-0.23%	-0.02%	0.17%	0.62%				
-0.08%	0.03%	0.14%	0.65%				
-0.26%	0.01%		0.54%	0.07%	-0.34%		
-0.04%	-0.11%	0.59%	0.69%	-0.04%	-0.37%	-0.13%	
-0.38%	-0.46%	0.21%		-0.03%	-0.66%	-0.13%	

Figure 6-8: Comparison of PARAGON2 and MCNP Assembly Pin Power Distributions for PQN-01 (15x15) Assembly Model

Figure 6-9 is a comparison of PARAGON2 and MCNP assembly pin power distributions for the PQN-02 (13x13) assembly model. The maximum difference between the two codes for this model was 0.92%.

13x13 Annular Pin Cell at HFP with no Boron

0.43%						
-0.17%	-0.61%					
-0.03%	-0.64%	-0.40%				
0.21%	0.32%	0.65%	0.72%			
0.06%	0.46%		0.39%	-0.47%		
0.30%	0.03%	0.51%	0.19%	-0.51%	0.03%	
-0.20%	-0.51%	-0.52%	-0.47%	-0.59%	0.53%	

13x13 Annular Pin Cell at HFP with 500ppm Boron

0.53%						
-0.04%	-0.56%					
-0.02%	-0.61%	-0.52%				
0.24%	0.19%	0.46%	0.69%			
0.19%	0.41%		0.49%	-0.49%		
0.00%	0.01%	0.32%	0.15%	-0.32%	0.11%	
-0.19%	-0.34%	-0.42%	-0.36%	-0.60%	0.44%	

13x13 Annular Pin Cell at HZP with no Boron

0.51%						
0.06%	-0.76%					
-0.17%	-0.64%	-0.45%				
-0.01%	0.14%	0.53%	0.92%			
-0.07%	0.43%		0.67%	-0.42%		
-0.05%	-0.02%	0.58%	0.14%	-0.48%	0.04%	
-0.05%	-0.39%	-0.46%	-0.26%	-0.46%	0.39%	

13x13 Annular Pin Cell at HZP with 500ppm Boron

0.45%						
0.06%	-0.58%					
0.05%	-0.45%	-0.43%				
0.11%	0.15%	0.28%	0.72%			
-0.06%	0.49%		0.54%	-0.46%		
0.13%	-0.04%	0.40%	0.15%	-0.39%	0.06%	
-0.11%	-0.30%	-0.58%	-0.40%	-0.50%	0.47%	

Figure 6-9: Comparison of PARAGON2 and MCNP Assembly Pin Power Distributions for PQN-02 (13x13) Assembly Model

Table 6-4 summarizes the maximum pin power differences between MCNP and PARAGON2 for all analyzed models. All maximum differences are below 1%. As can be seen, PARAGON2 was able to predict the pin power distributions in the assembly with a similar level of accuracy for both the solid pins and the annular pins.

Table 6-4: Maximum Deviations in the Comparison of Pin Power Distributions

Assembly Type	Power	Boron (ppm)	Maximum (1-P/M) (%)
Solid Fuel (17x17)	HFP	0	0.69
	HZP		0.70
PQN-01 (15×15)	HFP		0.80
	HZP		0.87
PQN-02 (13×13)	HFP		0.72
	HZP		0.92
Solid Fuel (17x17)	HFP	500	0.62
	HZP		0.70
PQN-01 (15×15)	HFP		0.72
	HZP		0.69
PQN-02 (13×13)	HFP		0.69
	HZP		0.72

6.2.3 Depletion

Figure 6-10 is a plot of the infinite multiplication factors versus burnup from modeling assembly depletion in PARAGON2. As can be seen, the initial eigenvalue is higher at the beginning of the depletion for the solid fuel, which indicates that a higher Uranium enrichment is needed for the initial reactivity of dual-cooled fuel to match that of the solid fuel. However, it is seen that as the models deplete, the annular fuel

eigenvalues achieve the same level as of the solid fuel and even overcomes it at high burnups.

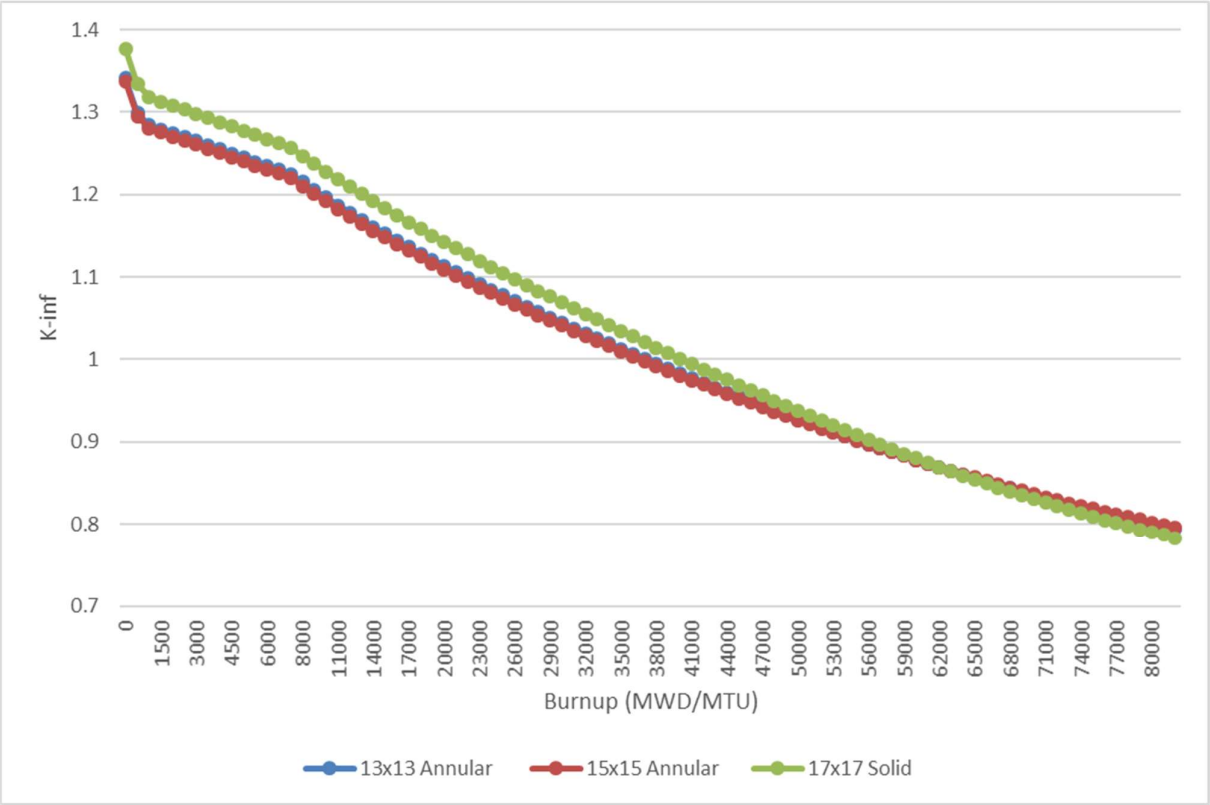

Figure 6-10: Eigenvalue assembly results of depletion model in PARAGON2

7 Conclusions

7.1 Conclusions

The objective of this research project was to study the effects of dual-cooling in annular fuel assembly neutronics while also assessing PARAGON2 capability of modeling this new type of fuel. For that, benchmarking was done against MCNP calculations.

A review of the current bibliography on dual-cooled annular fuel evidenced the lack of neutronic codes capable and verified for modeling such fuel type. The reason for this is that the equivalence relations for heterogeneous resonance integrals adopted in the existing codes were formulated only for solid cylindrical rods. Hence, the self-shielding effect in a dual-cooled fuel, which has water flowing in the inner channel, is not correctly calculated by them.

PARAGON2 is expected to be a viable option for such purpose. It employs an Ultra-Fine Energy Mesh Library (UFEML) with 6064 neutron and 97 gamma energy groups for multi-group cross section calculations. Doing so, the need for the resonance self-shielding calculation is eliminated.

Pin cell and assembly models were created using both PARAGON2 and MCNP6 codes. Not only did two different annular fuel lattices were studied (13x13 and 15x15), but also a standard solid fuel 17x17 lattice. The standard fuel model served as a reference of the current production result accuracy.

Models were created considering both poison-free moderator and 500ppm of soluble Boron in the moderator, in order to cover the effect of absorption in the inner region of the annular fuel and any potential code limitation on that aspect.

In the pin cell models, eigenvalue, radial power distribution and conversion ratio were assessed. In the assembly models, eigenvalue and pin power distribution were the parameters of interest. In all cases, comparison to MCNP6 results indicate that PARAGON2 is able to model dual-cooled fuel with the same level of accuracy it does standard solid fuel.

In addition, PARAGON2 results for dual-cooled fuel behaved much better when compared to all the benchmarks found in literature from other codes modeling such fuel, as shown in Table 5-2. For instance, benchmarks of CASMO-4 vs. MCNP-4C had almost 10% relative error on the conversion ratio and almost 3000 pcm error on the eigenvalue. In our study, the maximum error on the conversion ratio was below 4%, while the maximum error on the eigenvalues was below 250 pcm.

PARAGON2's accuracy in modeling dual-cooled fuel is derived from the fact that PARAGON2 does not perform any resonance self-shielding calculation. This calculation would involve equivalence relations that in most codes were formulated for solid cylindrical rods, where the material in the center of the rod is fuel and not water.

With that, one can conclude that PARAGON2 is a viable option for modeling dual-cooled annular fuel. PARAGON2 obtained results more accurate when modeling this fuel type than all other attempts found during the literature review of this project. In addition, they were within the proposed acceptance criteria which was defined based on engineering judgement.

Furthermore, the effects of the dual-cooling could be observed in the neutronics of the fuel. Due to the water presence inside of the annular fuel, the U-238 capture rate increased, which drove for higher values of conversion ratio and lower value of eigenvalue in the dual-cooled fuel compared to the standard solid fuel. The power gradient in the fuel of the DCF was also smaller than that of the solid fuel, given the moderation on the inner region of the annular fuel.

7.2 Vision of Future Work

7.2.1 Benchmark Higher Enrichment Cases

As in Section 6.2.3 it was observed that a higher Uranium enrichment was needed for the initial reactivity of dual-cooled fuel to match that of the solid fuel, it is recommended that analyses similar to the ones performed in this study are performed considering a higher enriched fuel.

7.2.2 Benchmark Depletion Results

Assembly and full core depletion results using PARAGON2 could be benchmarked against Monte Carlo codes which are able to model depletion accurately, such as SERPENT [55].

7.2.3 Formal PARAGON2 Qualification for the modeling of Dual-Cooled Annular Fuel

Should there be a need for Westinghouse to model this type of fuel some steps would need to be taken. PARAGON2's license application doesn't cover modeling Dual-Cooled Fuel. In order for it to do so, PARAGON2 would need to be formally qualified for this purpose. This qualification process with NRC would involve more benchmarks than the ones in this document, such the ones proposed in Sections 7.2.1 and 7.2.2, and comparisons to experimental data.

7.2.4 NEXUS Code Set Update

PARAGON is the core of NEXUS system, which is a much broader code set, as explained in Section 3. In this study, PARAGON inputs were manually modified to model the proposed geometries. However, for Westinghouse to be able to model this type of fuel using the NEXUS/ANC system, the other codes which interact with PARAGON would need to be updated to automatically create its input as needed and to read its output to create the correct cross-section data (CD) file.

It's worth mentioning that the current NEXUS is already able to model annular fuel, however only with vacuum in the center region. This would be the starting point for implementing the Dual-Cooled fuel modeling.

7.2.5 Full Core Analysis

The analyses performed in this study only cover pin cell and assembly models. Another analysis of interest is the full core one. Through the full core analysis, it's possible to evaluate core parameters such as the life cycle duration, peaking factors, shutdown margin and axial power distribution.

By evaluating these parameters, a better perspective can be obtained on how a core fueled with dual-cooled fuel compares to one with the standard solid fuel. Economical and safety aspects could be assessed for such evaluation.

In order to have the full core analysis performed based in the Westinghouse 3D core simulator (ANC), the update described in Section 7.2.4 would need to be addressed.

8 References

1. RHEE, Y. W., KIM, D. J., KIM, J. H., *et al.*. "Diametric Tolerance Control of Dual Cooled Annular Fuel Pellet without Inner Surface Grinding". In: **Proceedings of the Water Reactor Fuel Performance Meeting - WRFPM / Top Fuel 2009**, (p. 268). France

2. DOMINGUEZ, A. N., RAO, Y. "Modeling Approach for Annular-Fuel Elements using the ASSERT-PV Subchannel Code". In: **Proceedings of the 24th Nuclear Simulation Symposium**, 14 out. 2012. Ottawa, Ontario,14 October 2012. p. 11.

3. BUJAS, R. **Annular fuel element for high-temperature reactors**. Available at: https://patents.google.com/patent/US3928132A/en. Accessed on January 24, 2020. , 23 December 1975.

4. KAZIMI, M., HEJZLAR, P., CARPENTER, D., *et al.* **High Performance Fuel Design for Next Generation PWRs: Final Report**. Project DE-FG03-01SF22329., nº MIT-NFC-PR-082. Nuclear Energy Research Initiative (NERI), 2006.

5. SHEPHERD, D. A review of Accident Tolerant Fuel (ATF) concepts. In: **Scientific Basis of the Nuclear Fuel Cycle (SBNFM) - III Symposium at the European Materials Research Society (E-MRS) Spring Meeting**. May 11, 2015. Lille, France. DOI:10.13140/RG.2.2.24944.97287

6. SHEPHERD, D., ROSSITER, G., PALMER, I., *et al.* "Technology readiness level (TRL) assessment of advanced nuclear fuels". In: **TopFuel**, September 13, 2015. Zurich, Switzerland.

7. KOO, Y.-H., YANG, J. H., PARK, J.-Y., et al. "Status of Dual Cooled Annular Fuel Development in KAERI". In: **2013 EHPG Meeting**, 2013.

8. FENG, D., HEJZAR, P., KAZIMI, M. S.. "Thermal-Hydraulic Design of High-Power-Density Annular Fuel in PWRs". **Nuclear Technology**, Volume 160, Pages 16-44. 2007.

9. STEWART, C. W., CUTA, J. M., MONTGOMERY, S. D., *et al.* "**VIPRE-01 A Thermal-Hydraulic Code for reactor Cores**". Volumes 1-3, EPRI, NP-2511-CCM. July 1, 1985.

10. KWON, Y.-D., LEE, D.-S., YUN, T.-H. "Comparison of the Characteristics of Solid Type and Annular Type Nuclear Fuels Using Thermoelastic-Plastic-Creep FEM", **Mathematical Problems in Engineering**, v. 2016, p. 1–9, January 1, 2016. DOI: 10.1155/2016/1673107 [doi.org].

11. MOZAFARI, M. A., FAGHINI, F.. "Design of annular fuels for a typical VVER-1000 core: Neutronic investigation, pitch optimization and MDNBR

calculation". **Annals of Nuclear Energy**, Volume 60, October 2013, Pages 226-234. (2013).

12. ZAIDABADI, M., ANSARIFAR, G. R., ESTEKI, M. H. "Thermal hydraulic analysis of VVER-1000 nuclear reactor with dual-cooled annular fuel using K–ω SST Turbulence model", **Annals of Nuclear Energy**, v. 101, p. 118–127, 1 mar. 2017. DOI: 10.1016/j.anucene.2016.09.027 [doi.org].

13. HASSAN, A. A., EL-SHEIKH, B. M.. "Thermal Hydraulic Evaluation of a proposed annular fuel for VVER1000 Reactor". **J. Nucl. Tech. Appl. Sci.**, Vol. 6, No. 2, PP. 83 : 91. (2018).

14. KWON, H. et al. "Preliminary Thermal Hydraulic Design of SMR Core with 13 x 13 Annular Fuel Assemblies". In: **Transactions of the Korean Nuclear Society Spring Meeting**, Jeju, Korea, May 2019. Available at: https://www.kns.org/files/pre_paper/41/19S-346-%EA%B6%8C%ED%98%81.pdf. Accessed on January 20, 2020.

15. FENG, D. **Innovative Fuel Designs for High Power Density Pressurized Water Reactor**. Doctor of Philosophy (PhD) Thesis in Nuclear Science and Engineering, Department of Nuclear Engineering, Massachusetts Institute of Technology (MIT), p. 259, 2005.

16. FENG, D., MORRA, P., SUNDARAM, R., *et al.* "Safety Analysis of High-Power-Density Annular Fuel for PWRs", **Nuclear Technology**, v. 160, p. 45–62, 1 out. 2007. DOI: 10.13182/NT07-A3883 [doi.org]

17. LAHODA, E., FEINROTH, H., SALVATORE, M., *et al.* "High-Power-Density Annular Fuel: Manufacturing Viability", **Nuclear technology**, v. 160, p. 100–111, 1 out. 2007. DOI: 10.13182/NT07-A3886 [doi.org].

18. RHE, Y. W, et al.. "**Minimization of Inner Diametric Tolerance of Annular Pellet for Dual Cooled Fuel**". (INIS-XA--1074). International Atomic Energy Agency (IAEA). (2009).

19. Xu Z., Otsuka, Y., P. Hejzlar, et al., "High-Performance Annular Fuel Reactor Physics and Fuel Management", **Nuclear Technology**, Volume 160, Issue 1, Pages 63-79, (2007).

20. EDENIUS, M., et al.. "**CASMO-4, A Fuel Assembly Burnup Program, User's Manual**". Studsvik/SOA-95/1, Studsvik of America, Inc. (1995).

21. ANSARIFAR, G. R., ESTEKI, M. H., ZEIDABADY, M. "Investigation of the Dual-Cooled Annular Fuel Effect on the Thermal Power Uprate in a VVER-1000 Nuclear Reactor", **Nuclear Technology**, v. 195, 1 jul. 2016. DOI: 10.13182/NT15-90 [doi.org].

22. ZHAO, C.-Q., CAO, L., WU, H., *et al.* "Research on neutronics calculation method for SCWR with annular fuel", **Atomic Energy Science and Technology**, v. 50, n. 7, p. 1238–1244, 20 jul. 2016. DOI: 10.7538/yzk.2016.50.07.1238 [doi.org].

23. MAYHUE, L.; et al. "Qualification of NEXUS ANC Nuclear Design System for PWR Analyses". In: **Proc. Int. Conf. on Reactor Physics**, PHYSOR-2008, Interlaken, Switzerland, September 14-19, 2008.

24. ZHANG, B. "**Qualification of the NEXUS Nuclear Data Methodology**", WCAP-16045-NP-A, Addendum 1. November, 2005.

25. GEHIN, J. C.; GODFREY, A. T.; et al. "**Operational Reactor Model Demonstration with VERA: Watts Bar Unit 1 Cycle 1 Zero Power Physics Tests**". *In*: Consortium for Advanced Simulation of LWRs (CASL), CASL-U-2013-0105-001, Rev. 1, August, 2013. Available at: https://www.casl.gov/sites/default/files/docs/CASL-U-2013-0105-001_final.pdf. Accessed on March 24, 2019.

26. OUISLOUMEN, M.; HURIA, H. C.; MAYHUE, L. T.; et al. "**Qualification of the Two-Dimensional Transport Code PARAGON**". WCAP-16045-NP, Revision 0. March, 2003.

27. LIU, Y. S.; et al. "**ANC: A Westinghouse Advanced Nodal Computer Code",** WCAP-10966-A. Westinghouse Electric Company. September, 1986.

28. ZHANG, B. "**Pseudo Pin-by-Pin Calculation Methodology for Pin Power Recovery".** Doctor of Philosophy (PhD) Thesis in Nuclear Engineering, College of Engineering, The Pennsylvania State University, p. 140, 2010.

29. ZHANG, B., MAYHUE, L., HURIA, H., *et al.* "Development of 3D pseudo pin-by-pin calculation methodology in ANC". In: **International Conference on the Physics of Reactors 2012**, 1, January 1, 2012, Knoxville, Tennessee, USA, p. 64–76.

30. Westinghouse Electric Company, "**NEXUS/ANC9, The next-generation Westinghouse core design system**". Available at: http://smetona.net/Power/Ap1000.pdf. Accessed on March 24, 2019.

31. OUISLOUMEN, M.; BUECHEL, R. J., AOKI, S. "The Two-Dimensional Collision Probability Calculations in Westinghouse Lattice code: Methodology and Benchmarking". *In*: **Proc. Int. on the Physics of Reactors PHYSOR96**, Vol. 1, A366, Mito, Japan, 1996.

32. MACFARLANE, R.E. "**NJOY91.118: A code System For Producing Pointwise And Multigroup Neutron and Photon Cross Sections From ENDF/B Evaluated Nuclear Data**". ORNL, RSIC, PSR-171, 1994.

33. WOLTERS, E.; OUISLOUMEN, M.; MATSUMOTO, H.; "Effect of Pellet Radial Power and Temperature Distributions on Fuel Assembly Neutronics". *In*: **PHYSOR 2004 -The Physics of Fuel Cycles and Advanced Nuclear Systems: Global Developments**, Chicago, USA, April 25, 2004. p. 10.

34. STAMM'LER R.J.J, ABBATE M.J.,. "**Methods Of Steady-State Reactor Physics in Nuclear Design**". Academic Press, London. (1983).

35. OUISLOUMEN, M.; HURIA, H. C.; MAYHUE, L. T.; et al. "The new lattice code PARAGON and its qualification for PWR core applications". *In*: : **International conference on supercomputing in nuclear applications SNA'2003**, September 22, 2003, Paris, France.

36. YUAN, Y. "**The Design of High Power Density Annular Fuel for LWRs**". 2005. Doctor of Philosophy (PhD) Thesis in Nuclear Science and Engineering, Department of Nuclear Engineering, Massachusetts Institute of Technology (MIT), p. 255, 2005.

37. HEBERT, A.. "Isotropic Streaming Effects in Thermal Lattices". In: **Proc. ANS Int. Meeting on Mathematical Methods for Nuclear Applications**, September 2001, Salt Lake City, Utah, USA. (2001).

38. NGUYEN, T. Q. ; et al. "**Qualification of the PHOENIX-P/ANC Nuclear Design System for Pressurized Water Reactor Cores**". WCAP-11597-A, June, 1988.

39. OUISLOUMEN, M. "PARAGON2 Depletion Validation Using SERPENT2 Monte Carlo Code". *In*: **M&C 2017 - International Conference on Mathematics & Computational Methods Applied to Nuclear Science & Engineering**. Jeju, Korea. April 16-20, 2017, on USB (2017).

40. Westinghouse Electric Company. LTR-NRC-18-52 NP-Attachment. "**Slide Presentations for the 2018 Westinghouse Fuel Performance Update Meeting (Non-Proprietary)** ". July, 2018. Available at: https://www.nrc.gov/docs/ML1819/ML18197A427.pdf Accessed on January 10, 2020.

41. MACFARLANE, R. E., KAHLER, A. C. "Methods for Processing ENDF/B-VII with NJOY", **Nuclear Data Sheets**, Nuclear Reaction Data. v. 111, n. 12, p. 2739–2890, 1 dez. 2010. DOI: 10.1016/j.nds.2010.11.001 [doi.org]

42. OUISLOUMEN, Mohamed, OUGOUAG, A., GHRAYEB, S. "Anisotropic Elastic Resonance Scattering Model for the Neutron transport Equation", **Nuclear Science and Engineering**, v. 179, p. 59–84, 1 jan. 2015. DOI: 10.13182/NSE13-99 [doi.org]

43. REBELLO JR., A. L. P.. "**Estudo Paramétrico e Otimizacional de Alvos de Espalhamento para o Reator MYRRHA utilizando simulações em MCNPX e Redes Neurais**". B.S. final project in Nuclear Engineering, Federal University of Rio de Janeiro, Brazil, p.46. (2016).

44. X-5 Monte Carlo Team, "**MCNP – A General Monte Carlo N-Particle Transport Code, Version 5**". LA-UR-03-1987. (2008).

45. SHULTIS, J. K., and FAW, R. E.. "**An MCNP Primer**". Kansas State University, Manhattan. (2011).

46. Beacon, D. R.. "**Next Generation Reactor Core Analysis using Iterative Transport-Diffusion Methodology**". Master of Science Thesis in Nuclear

Engineering, College of Engineering, The Pennsylvania State University, p. 103. (2014).

47. GOORLEY, T.; et al. "**Initial MCNP6 Release Overview – MCNP6 Version 1.0**". LA-UR 13-22934. Available at: https://permalink.lanl.gov/object/tr?what=info:lanl-repo/lareport/LA-UR-13-22934. .

48. Los Alamos National Laboratory. "**MCNP USER'S MANUAL – Code version 6.2**". LA-UR-17-29981, October 27, 2017. Manual Rev. 0. (2017).

49. WHALEN, D. J., HOLLOWELL, D. E., and HENDRICKS, J. S. "**MCNP: Photon benchmark problems**". (No. LA-12196), Los Alamos National Laboratory, NM, United States. (1991).

50. GODFREY, A., FRANCESCHINI, F., PALMTAG, S., and STOUT, J. Analysis of Two-Dimensional Lattice Physics Verification Problems with MPACT. *In*: **Consortium for Advanced Simulation of LWRs (CASL CASL-U-2012-0172-000),** Rev. 0, December, 2012. Available at: https://www.casl.gov/sites/default/files/docs/CASL-U-2012-0172-000.pdf. Accessed on January 19, 2020.

51. BROWN, F.; et al. "**Reactor Physics Analysis with Monte Carlo**". LA-UR-10-02762. Available at: https://mcnp.lanl.gov/pdf_files/la-ur-10-02762.pdf. Accessed on January 19, 2020.

52. Cross Sections Evaluation Working Group. Report BNL-90365-2009 Rev.1. "**ENDF-6 Formats Manual - Data Formats and Procedures for the Evaluated Nuclear Data Files ENDF/B-VI and ENDF/B-VII**". July, 2010. Available at: https://www.oecd-nea.org/dbdata/data/manual-endf/endf102.pdf

53. MacFarlane, R. E.. "**An Introduction to the ENDF Formats**". LNS015012, Lectures given at the Workshop on Nuclear Data and Nuclear Reactors: Physics, Design and Safety. Trieste, 13 March – 14 April 2000. Available at: http://users.ictp.it/~pub_off/lectures/lns005/Number_1/MacFarlane_1.pdf

54. CHADWICK, M. B., HERMAN, M., OBLOŽINSKÝ, P., *et al.* "ENDF/B-VII.1 Nuclear Data for Science and Technology: Cross Sections, Covariances, Fission Product Yields and Decay Data", **Nuclear Data Sheets**, Special Issue on ENDF/B-VII.1 Library. v. 112, n. 12, p. 2887–2996, 1 dez. 2011. DOI: 10.1016/j.nds.2011.11.002 [doi.org].

55. LEPPÄNEN, J., PUSA, M., VIITANEN, T., *et al.* "The Serpent Monte Carlo code: Status, development and applications in 2013", **Annals of Nuclear Energy**, Joint International Conference on Supercomputing in Nuclear Applications and Monte Carlo 2013, SNA + MC 2013. Pluri- and Trans-disciplinarity, Towards New Modeling and Numerical Simulation Paradigms. v. 82, p. 142–150, August 1, 2015. DOI: 10.1016/j.anucene.2014.08.024 [doi.org].

56. OUISLOUMEN,O., et al. "**Qualification of the Two-Dimensional Transport Code PARAGON2**". WCAP-18443-NP. October, 2019.

APPENDIX A – PARAGON2 Input File

Below one can find an example of the PARAGON2 input file. This example is from an annular pin model from the 15x15 lattice geometry being modeled at HFP.

```
MODULE: General
   Title:      "PQN-01 15x15 Annular Pin Cell - 4.95 w/o Enr. - HZP"

MODULE: Library
   energy_groups      6064
   lib_file     prgnlib
   print_lib           -1

   composition     1
      mixture      1001  4.8585588E-02
                   8016  2.4292794E-02
                   5010  4.0278857E-06
      density     0.726735

   composition     2
      mixture     92235  1.1399753E-03
                  92238  2.1602364E-02
                  92234  1.0822287E-05
                  92236  3.3342097E-07
                  8016  4.5506991E-02
      density     8.988667

   composition     3
      mixture     40090  1.9591116E-02
                  40091  4.2913891E-03
                  40092  6.5379887E-03
                  40094  6.5989120E-03
                  40096  1.0585661E-03
                  50000  3.9319039E-04
                  26000  1.3296606E-04
                  8016  2.7626457E-04
                  24000  6.8006403E-05
                  14000  1.2588295E-05

   composition     4
      mixture     92235  1.1399753E-03
                  92238  2.1602364E-02
                  92234  1.0822287E-05
                  92236  3.3342097E-07
                  8016  4.5506991E-02
      density     8.988667

   composition     5
      mixture     92235  1.1399753E-03
                  92238  2.1602364E-02
                  92234  1.0822287E-05
                  92236  3.3342097E-07
                  8016  4.5506991E-02
      density     8.988667

   composition     6
      mixture     40090  1.9591116E-02
                  40091  4.2913891E-03
                  40092  6.5379887E-03
                  40094  6.5989120E-03
```

```
                40096  1.0585661E-03
                50000  3.9319039E-04
                26000  1.3296606E-04
                8016  2.7626457E-04
                24000  6.8006403E-05
                14000  1.2588295E-05

   composition     9
      mixture     13027  1.0000000E-06

MODULE: Temperature_table
   medium       1
      Temperature_unit  Kelvin
      Relative_power    0.00 0.25 0.50 0.75 1.00  2.00
      Burnup               0.0
         T_avg           900.00  900.00  900.00  900.00  900.00  900.00
         T_expansion     900.00  900.00  900.00  900.00  900.00  900.00
         92238           900.00  900.00  900.00  900.00  900.00  900.00
         94240           900.00  900.00  900.00  900.00  900.00  900.00
      Burnup              193.0
         T_avg           900.00  900.00  900.00  900.00  900.00  900.00
         T_expansion     900.00  900.00  900.00  900.00  900.00  900.00
         92238           900.00  900.00  900.00  900.00  900.00  900.00
         94240           900.00  900.00  900.00  900.00  900.00  900.00
      Burnup             1293.0
         T_avg           900.00  900.00  900.00  900.00  900.00  900.00
         T_expansion     900.00  900.00  900.00  900.00  900.00  900.00
         92238           900.00  900.00  900.00  900.00  900.00  900.00
         94240           900.00  900.00  900.00  900.00  900.00  900.00

   medium       2
      Temperature_unit  Kelvin
      Relative_power    0.00 0.25 0.50 0.75 1.00  2.00
      Burnup               0.0
         T_avg           900.00  900.00  900.00  900.00  900.00  900.00
         T_expansion     900.00  900.00  900.00  900.00  900.00  900.00
         92238           900.00  900.00  900.00  900.00  900.00  900.00
         94240           900.00  900.00  900.00  900.00  900.00  900.00
      Burnup              193.0
         T_avg           900.00  900.00  900.00  900.00  900.00  900.00
         T_expansion     900.00  900.00  900.00  900.00  900.00  900.00
         92238           900.00  900.00  900.00  900.00  900.00  900.00
         94240           900.00  900.00  900.00  900.00  900.00  900.00
      Burnup             1293.0
         T_avg           900.00  900.00  900.00  900.00  900.00  900.00
         T_expansion     900.00  900.00  900.00  900.00  900.00  900.00
         92238           900.00  900.00  900.00  900.00  900.00  900.00
         94240           900.00  900.00  900.00  900.00  900.00  900.00

   medium      11
      Relative_power    0.00 0.25 0.50 0.75 1.00 2.00
      Burnup               0.0
         T_avg           600.00  600.00  600.00  600.00  600.00  600.00
         T_expansion     600.00  600.00  600.00  600.00  600.00  600.00
         92238           600.00  600.00  600.00  600.00  600.00  600.00
         94240           600.00  600.00  600.00  600.00  600.00  600.00
      Burnup              193.0
         T_avg           600.00  600.00  600.00  600.00  600.00  600.00
         T_expansion     600.00  600.00  600.00  600.00  600.00  600.00
         92238           600.00  600.00  600.00  600.00  600.00  600.00
         94240           600.00  600.00  600.00  600.00  600.00  600.00
      Burnup             1293.0
         T_avg           600.00  600.00  600.00  600.00  600.00  600.00
         T_expansion     600.00  600.00  600.00  600.00  600.00  600.00
         92238           600.00  600.00  600.00  600.00  600.00  600.00
         94240           600.00  600.00  600.00  600.00  600.00  600.00
```

```
   medium      12
      Relative_power    0.00 0.25 0.50 0.75 1.00 2.00
      Burnup               0.0
         T_avg           600.00  600.00  600.00  600.00  600.00  600.00
         T_expansion     600.00  600.00  600.00  600.00  600.00  600.00
         92238           600.00  600.00  600.00  600.00  600.00  600.00
         94240           600.00  600.00  600.00  600.00  600.00  600.00
      Burnup              193.0
         T_avg           600.00  600.00  600.00  600.00  600.00  600.00
         T_expansion     600.00  600.00  600.00  600.00  600.00  600.00
         92238           600.00  600.00  600.00  600.00  600.00  600.00
         94240           600.00  600.00  600.00  600.00  600.00  600.00
      Burnup             1293.0
         T_avg           600.00  600.00  600.00  600.00  600.00  600.00
         T_expansion     600.00  600.00  600.00  600.00  600.00  600.00
         92238           600.00  600.00  600.00  600.00  600.00  600.00
         94240           600.00  600.00  600.00  600.00  600.00  600.00

   medium      21
      Relative_power    0.00 0.25 0.50 0.75 1.00 2.00
      Burnup               0.0
         T_avg           600.00  600.00  600.00  600.00  600.00  600.00
         T_expansion     600.00  600.00  600.00  600.00  600.00  600.00
         92238           600.00  600.00  600.00  600.00  600.00  600.00
         94240           600.00  600.00  600.00  600.00  600.00  600.00
      Burnup              193.0
         T_avg           600.00  600.00  600.00  600.00  600.00  600.00
         T_expansion     600.00  600.00  600.00  600.00  600.00  600.00
         92238           600.00  600.00  600.00  600.00  600.00  600.00
         94240           600.00  600.00  600.00  600.00  600.00  600.00
      Burnup             1293.0
         T_avg           600.00  600.00  600.00  600.00  600.00  600.00
         T_expansion     600.00  600.00  600.00  600.00  600.00  600.00
         92238           600.00  600.00  600.00  600.00  600.00  600.00
         94240           600.00  600.00  600.00  600.00  600.00  600.00

MODULE: Geometry
   Config_type           RECTANGULAR  1  1
   Pin_overlay

           2

   BC_type             REFL REFL REFL REFL
   print_geom             1
   Thermal_expansion     off
   Gaps                    0    0    0    0

   cell_type     2   (Standard Annular Fuel Cell)
      Cell_geometry      RECTANGULAR
      Meshx               1.431
      Meshy               1.431
      Radii               0.3365 0.3935 0.4000 0.5990 0.6050 0.6600
      Split_type             1    1    1    1    1    1
      Split_zone             1    1    1    1    1    1
      Sectors              none none none none none none quadrant-d
      Region_composition     1    6    9    5    9    6    1
      Temperature            21   11    12    1    12   11    21
      Burnup_BOL               0.00000
      Pin_Power_BOL            1.00000
      Coupling_order         3    3    3    3    1    1    1    1
      Boron_depletion     none none none none none none none
      Depletable_region     no   no   no   no   no   no   no
      Moderator_region      yes   no   no   no   no   no   yes

MODULE: Resonance
```

```
   resonance_pitch        1.431
   print_reso               0
   FP_scattering_matrix    no

MODULE: Flux
   Iteration               100  3  3  200  4  4
   SOR_parameters          1.3000 1.4000 1.0000
   Tolerance               2.0E-6  1.0E-3  5.0E-5
   TL_tolerance            1.0E-4  1.0E-2
   Initial_temperature_map     on
   Print_flux                  0

MODULE: Leakage
   Buckling                 0.00
   Criticality_search         ON
   Leakage_flag               ON
   Print_leakage               0

MODULE: Edit
   energy_groups           6030  6064
   power                 36.08822

   maps
      pin_power
      burnup

   group_constants
      energy_groups        6030  6064

MODULE: End
```

As one can see, the PARAGON input file is structured in modules. The “General” module is followed by the title for the case being modeled. The “Library” module specifies the cross-section library being used and defines the material mixtures being modeled, with its isotopes and number densities and the mixture density. The “Temperature_Table” module gives the temperatures for the material to be used. The “Geometry” module provides all the geometrical and physical information of the model being set up. The “Resonance” module provides the inputs for the resonance calculations (multi-group self-shielded cross-sections). The “Flux” modules provides the information on the neutron transport equation solution. The “Leakage” module defines the leakage spectrum correction on the fluxes. The “Edit” module allows the user to select what data to be printed out as output. One other module that was used to deplete the model in a few cases is the “Depletion” module. There are other modules available for usage in PARAGON but they were not of interest for this project.

APPENDIX B - MCNP Input File

Below one can find an example of the MCNP input file. This example is from an annular pin model from the 15x15 lattice geometry being modeled at HFP.

```
mcnp case for PQN-01 15x15 pwr annular pin cell with 4.95 w/o - 900K
c  Cell defintion Section...
c
c  Annular Fuel Cell contained in Universe 101
c
101    1    7.288241E-02   -31              imp:n=1   u=101
102    4    3.896099E-02    31  -32         imp:n=1   u=101
103    0                    32  -33         imp:n=1   u=101
104    3    6.826049E-02    33  -34         imp:n=1   u=101
105    0                    34  -35         imp:n=1   u=101
106    4    3.896099E-02    35  -36         imp:n=1   u=101
107    1    7.288241E-02    36              imp:n=1   u=101
c
c   Cell defining Global lattice filled with universe 101
c
801    1    7.288241E-02   -101  102  -103  104  -105  106
                          fill=101   imp:n=1.0
c
c    Outside of the square Assembly
c
804    0    #801   imp:n=0
c

c  Surface defintion Section
c
c   Cell boundaries
c
*101       px      0.7155
*102       px     -0.7155
*103       py      0.7155
*104       py     -0.7155
*105       pz      0.50
*106       pz     -0.50
c
c    Cylinder cards
c
c    Fuel cells, Guide Tube and Instrumentation tubes
c
31      cz     0.3365
32      cz     0.3935
33      cz     0.4000
34      cz     0.5990
35      cz     0.6050
36      cz     0.6600
c
c    Material definition section
c
c    Moderator Material  (updated from prgn_495_nodish.job)
c
m1      1001.01c 4.8585588E-02  8016.01c 2.4292794E-02  5010.00c 4.0278857E-06
c
c   S(alpha,beta) for Hydrogen in H2O
c
mt1    hh2o.01t
c
```

```
c   Fuel Region Material (updated from prgn_495_nodish.job)
c
m3     92235.22c 1.1399753E-03 92238.22c 2.1602364E-02 92234.22c 1.0822287E-05
       92236.22c 3.3342097E-07  8016.02c 4.5506991E-02
c
c   Clad of the Fuel Region
c
m4     40090.00c 1.9591116E-02 40091.00c 4.2913891E-03 40092.00c 6.5379887E-03
       40094.00c 6.5989120E-03 40096.00c 1.0585661E-03 50000.00c 3.9319039E-04
       26000.00c 1.3296606E-04  8016.01c 2.7626457E-04 24000.00c 6.8006403E-05
       14000.00c 1.2588295E-05
c
mode n
kcode     50000   1.12   50  2050
ksrc        .250      .250      .000
c
c    Temperatures in all the cells
c
tmp     5.1702E-08   7.7557E-08   5.1702E-08   7.7557E-08   5.1702E-08
        7.7557E-08   5.1702E-08   5.1702E-08
c
print
c
```